Astrophysical Constraints on Dense Matter in Neutron Stars

M. Coleman Miller

Abstract Ever since the discovery of neutron stars it has been realized that they serve as probes of a physical regime that cannot be accessed in laboratories: strongly degenerate matter at several times nuclear saturation density. Existing nuclear theories diverge widely in their predictions about such matter. It could be that the matter is primarily nucleons, but it is also possible that exotic species such as hyperons, free quarks, condensates, or strange matter may dominate this regime. Astronomical observations of cold high-density matter are necessarily indirect, which means that we must rely on measurements of quantities such as the masses and radii of neutron stars and their surface effective temperatures as a function of age. Here we review the current status of constraints from various methods and the prospects for future improvements.

1 Introduction

The nature of the matter in the cores of neutron stars is of great interest to nuclear physicists and astrophysicists alike, but its properties are difficult to establish in terrestrial laboratories. This is because neutron star cores reach a few times the density of matter in terrestrial nuclei and yet they are strongly degenerate and they have far more neutrons than protons. It thus occupies a different phase than is accessible in laboratories. Within current theoretical uncertainties there are many possibilities for the state of this matter: it could be primarily nucleonic, or dominated by deconfined quark matter, or mainly hyperons, or even mostly in a condensate.

Only astrophysical observations of neutron stars can constrain the properties of the cold supranuclear matter in their cores. Because we cannot sample the matter

M. Coleman Miller
Department of Astronomy and Joint Space-Science Institute, University of Maryland, College Park, MD 20742-2421, USA.
e-mail: miller@astro.umd.edu

directly, we need to infer its state by measurements of neutron star masses, radii, and cooling rates. For the last two of these, the method of measurement is highly indirect and thus subject to systematic errors. Note, to be precise, that throughout this review we mean by mass the gravitational mass (which would be measured by using Kepler's laws for a satellite in a distant orbit around the star) rather than the baryonic mass (which is the sum of the rest masses of the individual particles in the star); for a neutron star, the gravitational mass is typically less than the baryonic mass by $\sim 20\%$. We also mean by radius the circumferential radius, i.e., the circumference at the equator divided by 2π, rather than other measures such as the proper distance between the stellar center and a point on the surface. Again, for objects as compact as neutron stars, the difference can amount to tens of percent.

In this review we discuss current attempts to measure the relevant stellar properties. We also discuss future prospects for constraints including those that will come from analysis of gravitational waves. For each of the constraint methods, we discuss the current uncertainties and assess the prospects for lowering systematic errors in the future. In § 2 we set the stage by discussing current expectations from nuclear theory and laboratory measurements. In § 3 we examine mass measurements in binaries. In § 4 we discuss current attempts to measure the radii of neutron stars and show that most of them suffer severely from systematic errors. In § 5 we explore what can be learned from cooling of neutron stars, and the difficulties in getting clean measurements of temperatures. In § 6 we investigate the highly promising constraints that could be obtained from the detection of gravitational waves from neutron star–neutron star or neutron star–black hole systems. We summarize our conclusions in § 7. For other recent reviews of equation of state constraints from neutron star observations, see [105; 160; 181; 210; 23; 187; 117; 153; 92].

2 Expectations from Nuclear Theory

Any observations of neutron stars bearing on the properties of high-density matter must be put into the context of existing nuclear theory. This theory, which relies primarily on laboratory measurements of matter at nuclear density that has approximately equal numbers of protons and neutrons, must be extrapolated significantly to the asymmetric matter at far higher density in the cores of neutron stars. We also note that the inferred macroscopic properties of neutron stars depend on the nature of strong gravity as well as on the properties of dense matter (e.g., [167]), but for this review we will assume the correctness of general relativity.

In this section we give a brief overview of current thinking about dense matter. We begin with simple arguments motivating the zero-temperature approximation for the core matter and giving the basics of degenerate matter. We then address a commonly-asked question: given that the fundamental theory of quantum chromodynamics (QCD) exists, why can we not simply employ computer calculations (e.g., using lattice gauge theory) to determine the state of matter at high densities? Given that in fact such calculations are not practical, we explore the freedom that exists

in principle to construct models of high-density matter; the fundamental point is that because the densities are well above what is measurable in the laboratory, one could always imagine, in the context of a model, adding terms that are negligible at nuclear density or for symmetric matter but important when the matter is a few times denser and significantly asymmetric. After discussing some example classes of models, we survey current constraints from laboratory experiments and future prospects. We conclude with a discussion of how one would map an idealized future data set of masses, radii, temperatures, etc. of neutron stars onto the equation of state of cold dense matter.

2.1 The basics: dense matter and neutron stars

Consider a set of identical fermions (e.g., electrons or neutrons) of mass m and number density n. The linear space available to each fermion is thus $\Delta x \sim n^{-1/3}$, and the uncertainty principle states that the uncertainty in momentum (and hence the minimum momentum) is given by $\Delta p \Delta x \sim \hbar$ and thus $p_{\rm min} \sim \hbar n^{1/3}$, where $\hbar = 1.05457 \times 10^{-27}$ erg s is the reduced Planck constant. Done more precisely and assuming isotropic matter we find that this minimum is the Fermi momentum $p_F = (3\pi^2\hbar^3 n)^{1/3}$. The Fermi energy adds to the rest-mass energy via $E_{\rm tot} = (m^2c^4 + p_F^2c^2)^{1/2} = mc^2 + E_F$, and is $E_F \approx p_F^2/2m$ for $p_F \ll mc$ and $E_F \approx p_F c$ for $p_F \gg mc$, where $c = 2.99792458 \times 10^{10}$ cm s^{-1} is the speed of light.

Matter is degenerate when $E_F > kT$, and strongly degenerate when $E_F \gg kT$, where $k = 1.38065 \times 10^{-16}$ erg K^{-1} is the Boltzmann constant and T is the temperature. As a result, electrons (with their low masses $m_e = 9.109382 \times 10^{-28}$ g $= 0.510999$ MeV$/c^2$) become degenerate at much lower densities than do neutrons or protons. Matter dominated by nuclei heavier than hydrogen has ~ 2 baryons per electron, and hence electrons become relativistically degenerate ($p_F = m_e c$) at a density of $\approx 2 \times 10^6$ g cm^{-3}. In addition, above $\approx 2.5 \times 10^7$ g cm^{-3} the total energy of electrons becomes larger than $m_n c^2 - m_p c^2 = 1.294$ MeV, where $m_n = 1.674927 \times 10^{-24}$ g $= 939.566$ MeV$/c^2$ and $m_p = 1.672622 \times 10^{-24}$ g $= 938.272$ MeV$/c^2$ are respectively the rest masses of neutrons and protons. As a result, at these and greater densities electrons and protons can undergo inverse beta decay $e^- + p \rightarrow n + \nu_e$. At higher densities the ratio of neutrons to protons in nuclei increases, and then at the "neutron drip" density $\rho_{nd} \approx 4 \times 10^{11}$ g cm^{-3} neutrons are stable outside nuclei.

At infinite density, equilibrium matter consisting of just neutrons, protons, and electrons would have eight times as many neutrons as protons (and electrons, because charge balance has to be maintained). To see this, note that at infinite density all species are ultrarelativistic and their chemical potentials are thus dominated by their Fermi energies. Charge balance means that $n_p = n_e$, so equilibrium implies

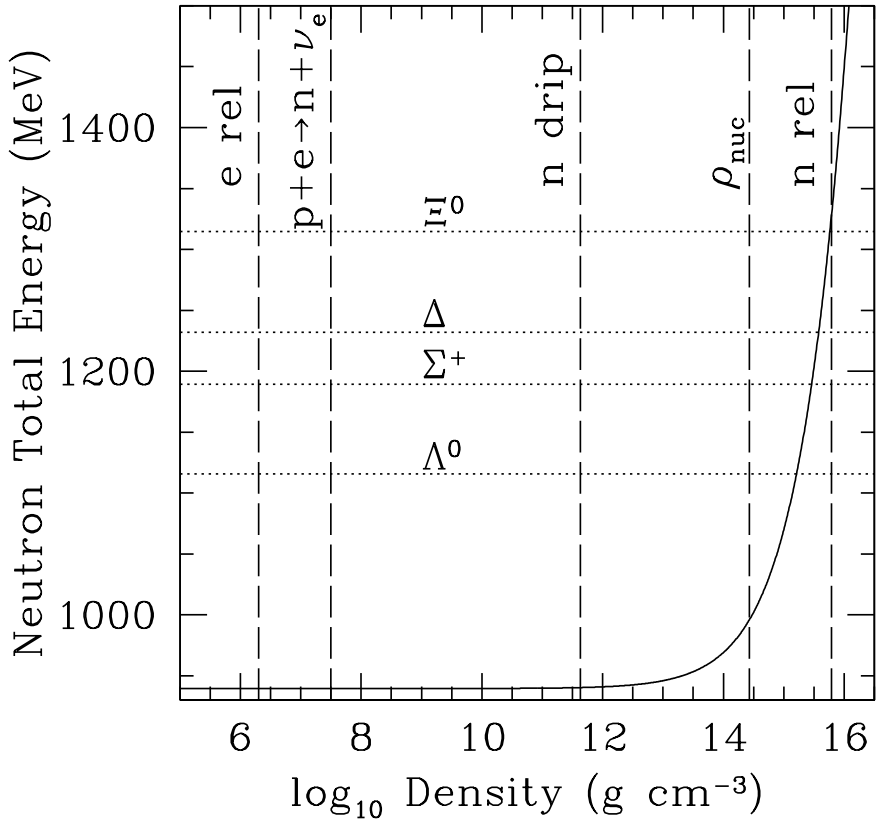

Fig. 1 Total energy per free neutron versus mass density (solid line). Above $\sim 10^{13}$ g cm^{-3} the Fermi energy starts to contribute palpably to the total, and above $\sim 10^{15}$ g cm^{-3} the total energy can exceed the rest mass energy of particles such as Λ^0, Σ^+, Δ, and Ξ^0 (marked by horizontal dotted lines). Interactions between these particles can change the threshold density. The central densities of realistic neutron stars range from $\sim 5\times10^{14}$ g cm^{-3} to $\sim$ few $\times 10^{15}$ g cm^{-3}, so some of these exotic particles may indeed be energetically favorable. Also marked are the densities at which free electrons become relativistic; where those electrons have enough total energy to make $p+e^-\rightarrow n+\nu_e$ possible; where free neutrons can exist stably; nuclear saturation density; and where free neutrons have a Fermi energy equal to their rest-mass energy. To calculate the neutron Fermi energy we assume that all the mass is in free neutrons; in reality at least a few percent of the mass is in protons and other particles, and below $\rho_{\rm nuc}$ a significant fraction of mass is in nuclei.

$$\begin{aligned} E_{F,n} &= E_{F,p} + E_{F,e^-} \\ &= 2E_{F,p} \\ n_n^{1/3} &= 2n_p^{1/3} \\ n_n &= 8n_p\ . \end{aligned} \tag{1}$$

For a neutron star with a canonical mass $M = 1.4\ M_\odot$ (where $M_\odot = 1.989 \times 10^{33}$ g is the mass of the Sun) and radius $R = 10$ km that for simplicity we will treat as made entirely of free neutrons, the average number density is $n = (M/m_n)/(4\pi R^3/3) = 4 \times 10^{38}$ cm^{-3}. This implies $p_F = 2.4 \times 10^{-14}$ g cm s^{-1} and thus $E_F \approx 2 \times 10^{-4}$ erg$=$ 100 MeV. This corresponds to a temperature of $T_F = E_F/k \approx 10^{12}$ K, which is much hotter than the expected interior temperatures $T < 10^{10}$ K typical of neutron stars more than a few years old [157]. Neutron stars are strongly degenerate.

Note, however, that the high Fermi energy of neutrons suggests the possibility of additional particles at high densities. For example, the lambda particle has a rest mass of $m_\Lambda = 1115.6$ MeV/c^2, so if the neutron Fermi energy exceeds 176 MeV then the lambda is in principle stable. Several other particles are within 300 MeV/c^2 of the neutron. In addition, because the density at the center of a neutron star is a few times nuclear saturation density $\rho_s \approx 2.6 \times 10^{14}$ g cm^{-3}, quarks may become deconfined or matter might transition to a state that is lower-energy than nucleonic matter even at zero pressure (strange matter; see, e.g., [69]). Various density thresholds are summarized in Figure 1.

Stars supported by nonrelativistic degeneracy pressure (a reasonable approximation for neutron stars, because $E_F < m_n c^2$) have radii that decrease with increasing mass in contrast to most other objects. To see this, consider a star with a mass M and radius R supported by nonrelativistic fermions of mass m. The Fermi energy per particle is $E_F \sim p_F^2/2m \sim \hbar^2 n^{2/3} \sim (M/R^3)^{2/3} \sim M^{2/3}/R^2$. The gravitational energy per particle is $E_G \sim -GMm/R$, where $G = 6.67 \times 10^{-8}$ g^{-1} cm^3 s^{-2} is Newton's gravitational constant, so the total energy per particle is $E_{\rm tot} = C_1 M^{2/3}/R^2 - C_2 M/R$ where C_1 and C_2 are constants. Minimizing with respect to R gives $R \sim M^{-1/3}$. Effects associated with interactions can change this slightly, but in practice most equations of state produce a radius that either decreases with increasing mass or is nearly constant over a broad range in mass. This led [118] to note that even for a star of unknown mass a measurement of the radius to within $\sim 10\%$ would provide meaningful constraints on the equation of state.

2.2 Models of matter at high densities

There are several classes of matter beyond nuclear density: ones in which neutrons and protons are the only baryons, ones in which other baryons enter (especially those with strange quarks), ones involving deconfined quark matter, and so on. Within each class there are a number of adjustable parameters, some of which are constrained by laboratory measurements at nuclear density or below but many of which can be changed to accommodate observations of neutron stars.

When confronted by this complexity a common question is: why is there uncertainty about dense matter? The fundamental theory, QCD, is well-established. Asymptotic freedom is not reached at neutron star densities, so the coupling constant is large enough that expansions similar to those in quantum electrodynamics

are not straightforward, but in principle one could imagine Monte Carlo calculations that establish the ground state of degenerate high-density matter.

This approach is unfortunately not currently practical, due to the lack of a viable algorithm for high baryon densities. This is because of the so-called "fermion sign problem", which has been known for many years. We start by considering a representative but small volume of matter at some density and chemical potential μ that can exchange energy and particles with its surroundings but has a fixed volume [98]. The thermodynamic state of the matter is therefore described by a grand canonical ensemble using a partition function

$$Z = Z(T,\mu) = \mathrm{Tr}\{\exp[-(\mathscr{H}-\mu N)/kT]\} \tag{2}$$

where $\mathscr{H}$ is the Hamiltonian and N is the particle number operator. It is common to use $\beta \equiv 1/(kT)$. The trace is evaluated over Fock space, which makes this formulation inconvenient. One can instead rewrite Z as

$$Z = \int \mathscr{D}A \, \mathrm{det}M(A) e^{-S_G(A)} \, , \tag{3}$$

that is, as a Euclidean functional integral over classical field configurations. Here A represents the degrees of freedom (quarks, gluons, ...), $S_G(A;\beta) = \int_0^\beta dx^4 \int d^3x \mathscr{L}_G^E(A)$ is the thermal Euclidean gauge action, and the quark propagator matrix is $M(A) = \not{D}(A) - m - \mu\gamma_4$ where $\not{D} = \gamma_\mu(\partial_\mu - igA_\mu^a t^a)$, t^a are the Hermitian group generators, g is the strong coupling constant, and γ are the Euclidean gamma matrices.

For a vanishing chemical potential $\mu = 0$, $\mathrm{det}M(A)$ is positive definite, meaning that all contributions add in the same direction and Z is comparatively straightforward to compute. If instead μ is real and nonzero, then $\mathrm{det}M(A)$ is complex in general. Thus although Z is still real and strictly positive, the integrands have various phases and the integral takes the form of a cancellation between large quantities. The bad news is that the general fermion sign problem is NP-hard [195], but work is proceeding on better approximation methods. If a first-principles evaluation of Z yields, without ambiguity, the equilibrium state of dense matter at low temperatures, then measurements of the properties of neutron stars would serve as important tests of QCD itself and would thus be probes of very fundamental physics indeed. Until that point, however, it is necessary to use phenomenological models.

It is very difficult to rule out an entire class of models (e.g., those with only nucleonic degrees of freedom or those with significant contributions from hyperons). This is because neutron star core densities and the asymmetry in the number densities of neutrons and protons are significantly greater than those that can be probed in laboratories. As a result, one could always imagine adding contributions that involve high powers of the density or asymmetry. These contributions would have a negligible impact on laboratory matter but would have important effects in the cores of neutron stars. One can make some general statements: for instance, if non-nucleonic components become important above some density the equilibrium radius at a given mass and the maximum mass both tend to be smaller than if only nucleonic degrees of freedom contribute (because the presence of a new energetically favorable

composition softens the equation of state). Unfortunately, it is difficult to establish a particular mass or radius that would eliminate such exotic models. For example, hyperonic models of neutron stars have been constructed with maximum masses $> 2.0\ M_\odot$ [112]. Nonetheless, although neutron star observations cannot entirely rule out model classes in principle, their role is important because they probe a different realm of matter than what is accessible in laboratories. Ockham's razor will then be used to judge between different model classes: if one class fits all data using a small number of parameters that have reasonable values and other classes require great complexity or unreasonable values, the first class would be preferred.

One basic category of models, relativistic mean field theories, is quite phenomenological in nature. In these models the degrees of freedom are nucleons and mesons (which couple minimally to the nucleons but the coupling could have some density dependence). The coupling strengths can be adjusted to laboratory data and/or neutron star observations. In a more microscopically oriented approach, one starts instead from some given nucleon-nucleon interaction (which can be extended to more than two nucleons) that is fitted to data including the binding energy of light nuclei and scattering data (for a recent effort in the context of chiral effective field theory, see [90]). In both approaches there is considerable freedom about the types of particles considered, e.g., the particles could be nucleons or the particles could include hyperons or deconfined quarks. We plot some mass-radius relations from representative equations of state in Figure 2. It is clear that models can be constrained tightly if more massive neutron stars are discovered, or if neutron star radii can be measured with accuracy and precision (especially for stars of known mass).

Constraints on the equation of state of cold dense matter can be obtained from astronomical observations or laboratory experiments. Some of the more useful experimental data come from relativistic heavy-ion collisions, which can reach 2 to 4.5 times nuclear saturation density [63] but which have relativistic temperatures and are therefore not degenerate. Laboratory data also include the binding energies of light nuclei and recent measurements of the neutron skin thickness of heavy nuclei such as ^{208}Pb ($0.33^{+0.16}_{-0.18}$ fm according to the PREX team [3]; see [164] for some of the implications of the expected more precise future measurements), which provide a rare glimpse of neutron-rich matter because the neutron wavefunctions extend slightly beyond the proton wavefunctions. These experiments thus measure the microphysics semi-directly, whereas all astrophysical observations place indirect constraints. In order to make explicit contact between microphysics and astrophysics we now discuss briefly how to construct models of neutron stars given a high-density equation of state.

2.3 Construction of neutron star models from microphysics

We argued earlier that the Fermi energy in the cores of neutron stars is much greater than the thermal energy. If we also assume that the matter is in its ground state at a given density, this implies that the pressure is only a function of density: $P = P(\rho)$

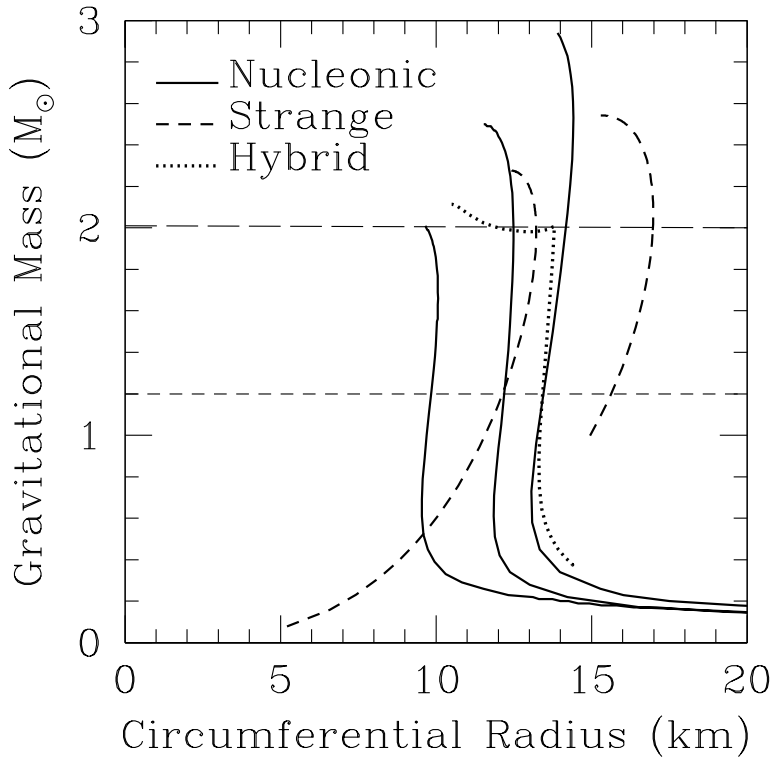

Fig. 2 Mass versus radius for nonrotating stars constructed using several different high-density equations of state. Rotation changes the radius to second order in the spin rate, but the corrections are minor for known neutron stars. The solid curves include only nucleonic degrees of freedom (these are the mass-radius relations for the soft, medium, and hard equations of state from [91]), the short dashed lines assume bare strange matter [109], and the dotted curve uses a hybrid quark equation of state with a phase transition [29]. The horizontal dashed line at 1.2 $M_\odot$ represents approximately the minimum gravitational mass for a neutron star in current formation scenarios, whereas the horizontal dashed line at 2.01 $M_\odot$ shows the highest precisely measured gravitational mass for a neutron star.

(this is called a *barotropic* equation of state). If we have such an equation of state we can compute the structure of a nonrotating and hence spherically symmetric star using the Tolman-Oppenheimer-Volkoff (TOV) equation [152]:

$$\frac{dP(r)}{dr} = -\frac{G}{r^2}\left[\rho(r) + \frac{P(r)}{c^2}\right]\left[M(r) + 4\pi r^3 \frac{P(r)}{c^2}\right]\left[1 - \frac{2GM(r)}{c^2 r}\right]^{-1} \quad (4)$$

where $M(r) = \int_0^r 4\pi\rho(r)r^2 dr$ is the gravitational mass integrated from the center to a circumferential radius r. Note that for $P/c^2 \ll \rho$ and $GM/c^2 \ll r$ this reduces to the Newtonian equation of hydrostatic equilibrium $dP/dr = -GM\rho/r^2$. Thus one can construct a model star by choosing a central density or pressure and integrating to the surface, which is defined by $P = \rho = 0$. This gives the radius and gravitational mass of the star. Similar constructions are possible for stars that rotate uniformly or differentially in some specified manner (see [56; 188]), but it is conceptually clearer to focus on the nonrotating case.

One can therefore determine the neutron star mass-radius relation from a given equation of state. If we suppose that in the future we will have precise measurements of the radii and gravitational masses of a large number of neutron stars, say from the minimum possible to the maximum possible mass, then comparison of the observed $M-R$ curve with predicted curves will strongly constrain the parameters of a given class of models. But is it possible to go in the other direction, that is, could one take observed (M,R) pairs and infer $P(\rho)$ directly while remaining agnostic about the microphysics that produces the equation of state?

This is not trivial. One might imagine that the construction of $P(\rho)$ would proceed as follows. First, we assume that we know the equation of state up to nuclear saturation density ρ_s. Even in this first step we therefore make an extrapolation from the nearly symmetric nuclear matter in nuclei to the highly asymmetric matter in neutron stars. We use this equation of state to compute the mass M_s and radius R_s of a star with a central density of ρ_s. We then observe a star with a slightly larger mass than M_s. The microscopic unknowns would be the central density (slightly larger than nuclear saturation) and the pressure at that density, which our two measurements (of M and R) are sufficient to constrain. We then bootstrap $P(\rho)$ by measuring the mass and radius of successively more massive neutron stars.

The difficulty with this procedure is evident from Figure 11 of [4], which shows that a star whose central density is exactly nuclear saturation density has a total mass of only $\sim 0.1\,M_\odot$. To get to the $M \approx 1.2\,M_\odot$ minimum for neutron star masses [151; 212] requires densities that are more than twice nuclear saturation. We will thus be required to extrapolate well beyond known matter in density and nuclear asymmetry to fit neutron star data. This is not fatal, because it means that we are simply comparing model predictions with data, but it does mean that $P(\rho)$ cannot be inferred blindly without models.

If additional assumptions are made, for example that between fiducial densities the equation of state is a polytrope $P \propto \rho^\gamma$, then [154] have shown that precise mass and radius measurements of as few as three neutron stars could suffice to give an empirically determined $P(\rho)$. The inferred $P(\rho)$ would then be compared with the predictions from microphysical equations of state. As discussed by [119], there are additional relatively model-independent constraints on the equation of state that one can infer from observations. For example, the typical radius of a neutron star scales as the quarter power of the pressure near nuclear satu-

ration density, and the maximum density that can be reached in a neutron star is $\rho_{\rm max} \approx 1.5 \times 10^{16}$ g cm$^{-3}(M_\odot/M_{\rm max})^2$ if the maximum mass is $M_{\rm max}$.

Our final note about the theoretical predictions is that there are some phenomena that have little effect on the mass-radius relation but are important for other observables. For example, the existence of a proton superconducting gap can modify core cooling dramatically [157], but the predicted gap energies of ~ 1 MeV [157] are so small compared to the Fermi energy that the overall structure of neutron stars will be affected minimally. Thus if neutron star temperatures and ages, particularly those of isolated neutron stars, can be inferred reliably, then they will provide a beautiful complement to the mass and radius measurements that are emphasized more in this review.

3 Constraints on Mass from Binary Observations

Mass measurements of neutron stars in binaries provide the most certain of all constraints on the properties of cold high-density matter, particularly when the companion to the neutron star is also a neutron star and thus the system approaches the ideal of two point masses. In this section we discuss such measurements, beginning with what can be learned from purely Newtonian observations and moving on to the greater precision and breaking of degeneracies that are enabled by measurements of post-Keplerian parameters from systems involving pulsars.

3.1 Newtonian observations of binaries

The classical approach to mass measurements in binaries assumes that one sees periodic variation in the energy of spectral lines from one of the stars in the binary, which we will call star 1. The period of variation is the orbital period $P_{\rm orb}$, the shape of the variation gives the eccentricity e of the orbit, and the magnitude K_1 (which has dimensions of speed) of the variation indicates the line-of-sight component of the orbital speed of star 1. Using Kepler's laws these observed quantities can be combined to form the "mass function", which for a circular orbit is

$$f_1(M_1,M_2) = \frac{K_1^3 P_{\rm orb}}{2\pi G} = \frac{M_2^3 \sin^3 i}{(M_1+M_2)^2} \, . \tag{5}$$

Here M_1 is the mass of the star being observed, M_2 is the mass of the other star, and i is the inclination of the binary orbit to our line of sight ($i = 0$ means a face-on orbit, $i = \pi/2$ means an edge-on orbit). From this expression, f_1 is the minimum possible mass for M_2; if $M_1 > 0$ or $i < \pi/2$ then $M_2 > f_1$. If periodically shifting spectral lines are also observed from the second star (and thus the binary is a so-

called double-line spectroscopic binary), then the mass ratio is known and only i is uncertain.

The inclination can be constrained for eclipsing systems. Particular precision is possible in some extrasolar planet observations because of the Rossiter-McLaughlin effect (in which the apparent color of the star varies in a way dependent on inclination as a planet transits across its disk; see [177; 135]). This effect also produces a velocity offset, which might have been seen in 2S 0921–63 [100]. The inclination can also be constrained in systems for which the companion to a compact object just fills its Roche lobe. This is because as the companion orbits it presents different aspects to us, and the amplitude of variation depends on the inclination; for example, a star in a face-on orbit looks the same to us at all phases, whereas star in an edge-on orbit varies maximally in its aspect [10; 134]. In practice this analysis is limited to systems that have low-mass companions (because Roche lobe overflow from a high-mass companion to a lower-mass compact object is usually unstable; see [73]) and that have transient accretion phases and hence have long intervals in which there is effectively no accretion disk (because an active accretion disk easily outshines a low-mass star and thus the binary periodicity is very difficult to observe). Neutron star X-ray binaries might be less likely to be transient than black hole X-ray binaries, and their companions tend to be much less massive and hence dimmer than the companions to black holes [73]. Thus despite the great success of this method for black hole binaries it has found limited application for neutron star binaries.

3.2 Post-Keplerian measurements of pulsar binaries

The most precise measurements of the masses of neutron stars in binaries are made for systems in which additional parameters can be measured. The extreme timing precision of pulsars makes pulsar binaries especially good candidates for such measurements. The new effects that can be measured are:

- Precession of the pericenter of the system, $\dot{\omega}$.
- Einstein delay γ. At pericenter, the gravitational redshift from the system is maximized, as is the special relativistic redshift because the orbital speed is highest at pericenter.
- Binary orbital decay $\dot{P}_b$. Gravitational waves are emitted by anything that has a time-variable quadrupole (or higher-order) mass moment. This shrinks and circularizes binary orbits.
- Shapiro delay, r and s. When the signal from the pulsar passes near its companion, time dilation in the enhanced potential delays the signal compared to the arrival time of a photon in flat spacetime. The magnitude of the delay over the orbit is characterized by the range r and shape s of the delay as a function of phase. See [75] for a recent reparameterization of the Shapiro delay that may represent the error region better for some orbital geometries.

Using the notation of [74], the dependences of these post-Keplerian parameters on the properties of the binary are

$$\begin{aligned}
\dot{\omega} &= 3\left(\tfrac{P_b}{2\pi}\right)^{-5/3}(T_\odot M)^{2/3}(1-e^2)^{-1} \\
\gamma &= e\left(\tfrac{P_b}{2\pi}\right)^{1/3} T_\odot^{2/3} m_c(m_p+2m_c) \\
\dot{P}_b &= -\tfrac{192\pi}{5}\left(\tfrac{P_b}{2\pi}\right)^{-5/3} f(e) T_\odot^{5/3} m_p m_c M^{-1/3} \\
r &= T_\odot m_2 \\
s &= \sin i
\end{aligned} \tag{6}$$

where m_p is the pulsar mass, m_c is the companion mass, $M = m_p + m_c$ is the total mass, $T_\odot = GM_\odot/c^3 = 4.925590947\mu$s, and $f(e) = (1+73e^2/24+37e^4/96)(1-e^2)^{-7/2}$. For a given system, there are thus three Keplerian parameters that can be measured (binary period, radial velocity, and eccentricity) along with the five post-Keplerian parameters. For a system such as the double pulsar J0737–3039A/B [41] additional quantities can be measured. Hence double neutron star systems in which at least one is visible as a pulsar are superb probes of general relativity and yield by far the most precise masses ever obtained for any extrasolar objects.

As discussed by [74], the neutron stars with the greatest timing precision are the millisecond pulsars. These, however, are spun up by accretion in Roche lobe overflow systems, and that accretion also circularizes the system to high precision. As a result, precession of the pericenter and the Einstein delay cannot be measured. The Shapiro delay, however, can be measured even for circular binaries, and because the Shapiro delay does not have classical contributions from tides (unlike pericenter precession, for example), r and s can yield unbiased mass estimates. As pointed out by Scott Ransom, Shapiro delay measurements are likely to become more common due to the development of very high-precision timing for gravitational wave detection via pulsar timing arrays. The consequence is that currently the most constrained systems are field NS-NS binaries, in which little mass transfer has taken place in the system and the stars are thus close to their birth masses. In contrast, recycled millisecond pulsars have had an opportunity to acquire an additional several tenths of a solar mass via accretion.

Another possibility, which is described clearly by [74], is that in high stellar density environments such as globular clusters binary-single interactions could play a major role. For example, a pulsar could be recycled to millisecond periods and then an exchange interaction could leave it in an eccentric binary with a white dwarf or another neutron star. Such a system would have a measurable $\dot{\omega}$ and γ, and the neutron star could be high-mass and have excellent timing precision.

We do note that there are two drawbacks to NS-WD systems in globulars compared to field NS-NS systems. First, although white dwarfs are small they are not point masses to the degree that neutron stars are. As a result, there is a small contribution to the precession from the finite structure of the white dwarfs. Second, even at the high stellar densities of globulars a comparatively large orbit is required for there to be a significant probability of interaction. To see this, note that the rate of interactions for a binary of interaction cross section σ is $\tau^{-1} = n\sigma v$, where n is the

number density of stars (typically in the core $n = 10^{5-6}$ pc^{-3}) and $v \sim 10$ km s^{-1} is the velocity dispersion. For a system of mass M, the interaction cross section for a closest approach of a, roughly equal to the semimajor axis of the binary, is $\sigma \approx \pi a(2GM/v^2 + a)$. If $M \approx 2\ M_\odot$ and $n = 10^5$ pc^{-3}, this implies $\tau = 10^{10}$ yr when $a \approx 0.04$ AU. This implies orbital periods greater than a day, so dynamically formed NS-WD binaries are systematically larger than NS-NS binaries formed in situ. Thus longer observation times are required to achieve a given precision.

3.3 Dynamically estimated neutron star masses and future prospects

For a recent compilation of dynamically estimated neutron star masses and uncertainties, see [104]. From the standpoint of constraints on dense matter, the most important development over the last few years has been the discovery of neutron stars with masses $M \sim 2\ M_\odot$, and possibly more. The first such established mass was for PSR J1614–2230. Demorest et al. [65] determined that its mass is $M = 1.97 \pm 0.04\ M_\odot$, which they obtained via a precise measurement of the Shapiro delay. This measurement was aided by the nearly edge-on orientation of the system (inclination angle 89.17°), which increases the maximum magnitude of the delay and produces a cuspy timing residual that is easily distinguished from any effects of an eccentric orbit.

The second large mass that has been robustly established belongs to PSR J0348+0432. Antoniadis et al. [8] observed gravitationally redshifted optical lines from the companion white dwarf. The observed Doppler modulation of the energy of these lines yields a mass ratio when combined with the modulation of the observed spin frequency of the pulsar. In addition, interpretation of the Balmer lines from the white dwarf in the context of white dwarf models gives a precise mass for the white dwarf, and indicates that the neutron star has a mass of $M = 2.01 \pm 0.04\ M_\odot$.

In addition to these well-established high masses, there are hints that some black widow pulsars (those that are currently evaporating their companions) might have even higher masses. This was first reported for the original black widow pulsar PSR B1957+20 [201]. For this star the best-fit mass is $M = 2.40 \pm 0.12\ M_\odot$, but at the highest allowed inclination and lowest allowed center of mass motion the mass could be as low as 1.66 $M_\odot$. More recently, [172] analyzed the gamma-ray black widow pulsar PSR J1311–3430 and found a mass of $M = 2.7\ M_\odot$ for simple heated light curves (but with significant residuals in the light curve), and no viable solutions with a mass less than 2.1 $M_\odot$. They conclude that better modeling and more observation is needed to establish a reliable mass, but it is an intriguing possibility that black widow pulsars have particularly large masses.

From the astrophysical standpoint, it has been proposed that neutron star birth masses are bimodal, depending on whether the core collapse occurs due to electron capture or iron core collapse [180]. There is also mounting evidence for systematically higher masses in systems that are expected to have had substantial accretion

[216]. From the standpoint of nuclear physics, [120] point out that 2.0 $M_\odot$ neutron stars place interesting upper limits on the physically realizable energy density, pressure, and chemical potential. Higher masses would present even stronger constraints.

To a far greater extent than with the other constraints described in this review, we can be confident that the mere passage of time will greatly improve the mass measurements, and indeed all of the timing parameters. Table II of [62] shows that as a function of the total observation time T (assuming a constant rate of sampling), the fractional errors in the post-Keplerian parameters scale as $\Delta\dot{\omega} \propto T^{-3/2}$, $\Delta\gamma \propto T^{-3/2}$, $\Delta\dot{P}_b \propto T^{-5/2}$, $\Delta r \propto T^{-1/2}$, and $\Delta s \propto T^{-1/2}$; for the r and s parameters the improvements are simply due to having more measurements, whereas the others improve faster with time because the effects accumulate. Particularly good improvement is expected for the NS-WD systems because as we describe above they have larger orbits and thus slower precession than NS-NS systems. There is thus reason to hope that additional high-mass systems will be discovered.

There are also planned observatories and surveys that will dramatically increase the number of known pulsars of all types, which will likely include additional NS-NS and NS-WD systems. An example of such a planned observatory is the Square Kilometer Array, which has been projected to increase our known sample of pulsars by a factor of ~ 10. In addition, as [194] pointed out recently, future high-precision astrometry will be able to deconvolve the parallactic, proper, and orbital motion of the two components of a high-mass X-ray binary. They estimate that for parameters appropriate to the Space Interferometry Mission this will yield a neutron star mass accurate to 2.5% in X Per, to 6.5% in Vela X-1, and to $\sim$10% in V725 Tau and GX 301–2.

It is thus probable that in the next ~ 10 years we will have far more, and far better, estimates of the masses of individual neutron stars. We do not, however, have a guarantee that any of those masses will be close to the maximum allowed. We thus need additional ways to access the properties of high-density matter. In particular, many equations of state imply similar maximum masses but widely different radii. We therefore turn to constraints on the radius.

4 Constraints on Radius, and Other Mass Constraints

As discussed in § 2, accurate measurements of the radii of neutron stars would strongly constrain the properties of neutron star core matter. Unfortunately, all current inferences of neutron star radii are dominated by systematic errors, and hence no radius estimates are reliable enough for such constraints. However, future measurements using the approved mission NICER [81] and the proposed missions LOFT [70], AXTAR [169], and ATHENA+ [149] hold great promise for precise radius measurements if the effects of systematic errors can be shown to be small. In this section we discuss various proposed methods for measuring radii and the di-

verse results obtained by applying these methods. Some of the methods also result in mass estimates, so we discuss those implications along the way.

4.1 Thermonuclear X-ray bursts

More than thirty years ago it was proposed that the masses and radii of neutron stars could be obtained via measurement of thermonuclear X-ray bursts [203]. These bursts occur when enough hydrogen or helium (or carbon for the long-lasting "superbursts") accumulates on a neutron star in a binary. Nuclear fusion at the base of the layer becomes unstable, leading to a burst that lasts for seconds to hours. For a selection of observational and theoretical papers on thermonuclear bursts, see [82; 19; 213; 101; 113; 191; 76; 77; 192; 125; 185; 57]. In some bursts, fits of a Planck function to the spectra reveal a temperature that initially increases, then decreases, then increases again before finally decreasing [124; 96; 184]. These are called photospheric radius expansion (PRE) bursts. The usual assumption is that PREs occur because the radiative luminosity exceeds the Eddington luminosity

$$L_E = \frac{4\pi GMc}{\kappa} \tag{7}$$

where M is the mass of the star and κ is the radiative opacity. At luminosities greater than L_E, an optically thick wind can be driven a potentially significant distance from the star. This leads to an increase in the radiating area and a consequent decrease in the temperature [155; 67]. For Thomson scattering in fully ionized matter with a hydrogen mass fraction X, $\kappa = 0.2(1+X)$ cm^2 g^{-1} and thus

$$L_E = 2.6 \times 10^{38} \text{ erg s}^{-1}(1+X)^{-1}(M/M_\odot) \, . \tag{8}$$

The basic method of [203] involves several assumptions. These are:

1. The full surface radiates uniformly after the photosphere has retreated to the radius of the star.
2. The stellar luminosity is the Eddington luminosity at the point of "touchdown", which is defined as the time after the peak inferred photospheric radius is reached when the color temperature, derived from a Planck fit to the spectrum, is maximal. The luminosity can then be determined via measurement of the flux at Earth and the distance to the star, assuming that the flux is emitted isotropically.
3. The spectral model for the atmosphere is correct. Thus the model must have been verified against data good enough to distinguish between models, and the atmospheric composition must be known. It is typically assumed that the color factor $f_c \equiv T_{\rm col}/T_{\rm eff}$, which is the ratio between the fitted Planck temperature and the effective temperature, is not only known but is constant throughout the cooling phase.
4. All other sources of emission from the system are negligible.

Using these assumptions, and using the notation of [187], if we have measured the distance D to the star and know κ, we can measure the touchdown flux

$$F_{\rm TD,\infty} = \frac{GMc}{\kappa D^2}\sqrt{1-2\beta(r_{\rm ph})} \tag{9}$$

where $\beta(r) \equiv GM/rc^2$, the factor before the square root is the Eddington flux diluted by distance, and $r_{\rm ph}$ is the radius of the photosphere. We can also use the cooling phase of the burst to define a normalized angular surface area

$$A = \frac{F_\infty}{\sigma_{\rm SB} T_{\rm col,\infty}^4} = f_c^{-4}\left(\frac{R}{D}\right)^2 (1-2\beta)^{-1}\,. \tag{10}$$

Here $\sigma_{\rm SB} = 5.6704\times10^{-5}$ erg cm^{-2} s^{-1} K^{-4} is the Stefan-Boltzmann constant and F_∞ and $T_{\rm col,\infty}$ are the flux and fitted Planck temperature that we measure in the cooling phase. Then the combinations of observed quantities

$$\begin{aligned} \alpha &\equiv \tfrac{F_{\rm TD,\infty}}{\sqrt{A}}\tfrac{\kappa D}{c^3 f_c^2} \\ \gamma &\equiv \tfrac{Ac^3 f_c^4}{F_{\rm TD,\infty}\kappa} \end{aligned} \tag{11}$$

can be related to β and R by $\alpha = \beta(1-2\beta)$ and $\gamma = R[\beta(1-2\beta)^{3/2}]^{-1}$ and solved to yield

$$\begin{aligned} \beta &= \tfrac{1}{4} \pm \tfrac{1}{4}\sqrt{1-8\alpha}\,, \\ R &= \alpha\gamma\sqrt{1-2\beta}\,, \\ M &= \beta R c^2/G\,. \end{aligned} \tag{12}$$

The problem is that for several bursters, the most probable values of the observationally inferred quantities $F_{\rm TD,\infty}$, A, and D, combined with the model parameter f_c, yield $\alpha > 1/8$. This would imply that the mass and radius are complex numbers. For example, in their analysis of 4U 1820–30, [86] used a Gaussian prior probability distribution for $F_{\rm TD,\infty}$, which had a mean $F_0 = 5.39\times10^{-8}$ erg cm^{-2} s^{-1} and a standard deviation $\sigma_F = 0.12\times10^{-8}$ erg cm^{-2} s^{-1}. They also used a Gaussian prior probability distribution for A, with $A_0 = 91.98$ (km/10 kpc)^2 and $\sigma_A = 1.86$ (km/10 kpc)^2. Their prior probability distribution for D was a boxcar distribution with a midpoint $D_0 = 8.2$ kpc and a half-width of $\Delta D = 1.4$ kpc. Finally, they assumed a boxcar prior probability distribution for the color factor, with $f_{c0} = 1.35$ and a half-width $\Delta f_c = 0.05$. If we take the midpoint of each distribution and also follow [86] by assuming that the opacity is dominated by Thomson scattering and thus $\kappa = 0.2$ cm^2 g^{-1} for the pure helium composition appropriate to 4U 1820–30, we find $\alpha = 0.179 > 1/8$.

[86] note that the probability of obtaining a viable M and R for 4U 1820–30 from these equations drops with increasing distance, but if we reduce D to the 6.8 kpc, which is the smallest value allowed in the priors of [86], and keep the other input parameters fixed, we find $\alpha = 0.148$. If we also increase f_c to its maximum value of 1.4 and take the $+2\sigma$ value of A and the -2σ value of $F_{\rm TD,\infty}$, α is still 1.29. In

fact [187] showed that if we consider the prior probability distribution of $F_{\rm TD,\infty}$, A, D, and f_c used by [86], only a fraction 1.5×10^{-8} of that distribution yields real numbers for M and R. This demonstrates that the 4% fractional uncertainties on the mass and radius of this neutron star obtained by [86] emerge from the theoretical assumptions rather than from the data. Thus such apparent precision is actually a red flag that one or more of the model assumptions is incorrect.

The first suggestion for which assumption is in error came from [187], who proposed that although the entire surface still emits uniformly throughout the cooling phase, the photospheric radius might be larger than the radius of the star, i.e., $r_{\rm ph} > R$. However, analysis of the cooling phase of the superburst from 4U 1820–30 [142] demonstrates that such a solution is disallowed for at least the superburst emission from this star, because any detectable change in photospheric radius would require a flux very close to Eddington, and such fluxes give extremely poor fits to the data. The work of [142] used and verified the fully relativistic Comptonized spectral models of [190], and also showed that the *fraction* of the surface that emits changes systematically throughout the superburst (the emitting area drops by $\sim 20\%$ during the $\sim$1600 seconds analyzed). Moreover, there is no guarantee that the whole surface was emitting at *any* time. Thus the star does not emit uniformly over its entire surface during the superburst, and hence it cannot be assumed that it has uniform emission during shorter bursts when the data quality is insufficient to check this assumption. Indeed, the presence of burst oscillations (see [208] for a recent review) demonstrates that there is nonuniformity in burning during many bursts. Additional concerns are that the color factor is likely to evolve during the burst, and that some of the bursts are not fit well using existing spectral models [37; 189; 48; 217; 78; 80].

Suleimanov et al. [189] find a radius of more than 14 km from a long PRE burst from 4U 1724–307 based on fits of their spectral models to the decaying phase of the burst. As part of their fits, they find that the Eddington flux occurs not at touchdown, but at a 15% lower luminosity; this, therefore, calls into question another of the assumptions in the standard approach to obtaining mass and radius from bursts. Their radius value is based on the good fit they get to the bright portion of the burst, when according to their fits the local surface flux exceeds $\sim 50\%$ of Eddington. This is an intriguing method that should be considered carefully when data are available from the next generation of X-ray instruments. However, a potential concern is that the spectra does not agree with their models below $\sim 50\%$ of Eddington. This suggests that there is other emission in the system at least at those lower luminosities, and hence that some of this emission might be present at higher luminosities as well. Against this is the excellent fit without extra components that [142] obtained for the superburst from 4U 1820–30 using the models of [190]. More and better data are the key.

If truly excellent spectra can be obtained, then as pointed out by [131], inference of the surface gravity g and surface redshift z leads uniquely to determination of the stellar mass and radius. However, even the $\sim 2 \times 10^7$ counts observed using *RXTE* from the 4U 1820–30 superburst are insufficient to determine both g and z uniquely [142], so this appears to require much larger collection areas. The combination $(1+z)/g^{2/9}$ can be measured precisely using sufficiently good continuum spectra, and

then combined with other measurements to, possibly, constrain M and R [142; 126], so this is promising for the future. The net result is that currently inferred masses and radii from spectral fits to thermonuclear X-ray bursts must be treated with caution; none are currently reliable enough to factor into equation of state constraints.

4.2 Fits of thermal spectra to cooling neutron stars

In principle, observations of cooling neutron stars with known distances allow us to measure the radii of those stars, modulo an unknown redshift. In practice, as with radius estimates from bursts, systematic errors dominate and thus current radius determinations are not reliable enough to help constrain the properties of dense cold matter.

To understand the basic principles, suppose that the star is at a distance d and that we measure a detector bolometric flux $F_{\rm det,bol}$ from the star that is fit by a spectrum with an effective temperature $T_{\rm eff,\infty}$ at infinity. Suppose that we also assume that the entire surface radiates uniformly and isotropically. If the surface redshift is z then the luminosity at the surface is $L_{\rm surf} = (1+z)^2 L_\infty = (1+z)^2 F_{\rm det,bol} 4\pi d^2 = 4\pi R^2 \sigma_{\rm SB} T_{\rm surf}^4 = 4\pi R^2 (1+z)^4 \sigma_{\rm SB} T_{\rm eff,\infty}^4$. This implies

$$R = (1+z)^{-1} d [F_{\rm det,bol}/(\sigma_{\rm SB} T_{\rm eff,\infty}^4)]^{1/2} \, . \tag{13}$$

The key questions are therefore (1) how well can the distance be determined, (2) how well can $T_{\rm eff,\infty}$ be established, given that it depends on a spectral fit, and (3) how well is the flux known, since only the thermal component is relevant?

There are two categories of sources that have been studied carefully in this manner to estimate neutron star radii. The first is the so-called quiescent low-mass X-ray binaries (qLMXBs). These are transiently accreting neutron stars that, in the ideal case, do not accrete at all when they are not accreting actively. Some qLMXBs are in globular clusters, so for those sources the distance to the qLMXBs can be determined by measuring the distance to the cluster. If a qLMXB has a phase of active accretion, then it has a steady supply of hydrogen or helium, which should rise to the top and dominate the surface composition after a few seconds [5]. In addition, the dipolar magnetic field strengths of LMXBs are weak, typically $\sim 10^8 - 10^9$ G averaged over the surface [36]. Thus magnetic effects will be minimal (note that magnetic fields can affect energy spectra significantly at photon energies comparable to or less than the electron cyclotron energy $\hbar\omega_B = \hbar eB/m_e c = 11.6\,{\rm keV}(B/10^{12}\,{\rm G})$). Therefore, the spectra might be well-modeled by nonmagnetic atmospheres. These characteristics are all good for estimating radii. [85] recently applied this method to five qLMXBs in globular clusters. They assumed that all the stars have the same radius, that the atmospheres are nonmagnetic and composed purely of hydrogen (an assumption that they supported on the basis of the companion type in two cases), and that the surface emission was uniform. With these assumptions, they found $R = 9.1^{+1.3}_{-1.5}$ km.

However, the atmospheric composition matters greatly. For example, [182] find that whereas fits of hydrogen atmospheres to a qLMXB in the globular cluster M28 yield a radius of $R = 9 \pm 3$ km at 90% significance, a helium atmosphere gives $R = 14^{+3}_{-8}$ km with an equally good fit ($\chi_\nu/\mathrm{dof} = 0.87/141$ for the H atmosphere, 0.88/142 for the He atmosphere). Similarly, [46] fit data from a qLMXB in the globular cluster M13 and find $R = 9.0^{+3.0}_{-1.5}$ km for an H atmosphere and $R = 14.6^{+3.5}_{-3.1}$ km for a He atmosphere, again with a comparable quality of fit. Although one might argue [85] that if the companion is hydrogen rich the neutron star atmosphere will be as well, it has been proposed that after $\sim 10^{2-4}$ years diffusive burning of hydrogen will leave helium as the main surface composition ([49; 50]; see [22] for the first step in a re-evaluation of this work in the light of a better treatment of Coulomb separation of ions). Given that ~ 15 years of RXTE observations have not revealed any accretion-powered outbursts from any of the qLMXBs included in the analysis of [85], the recurrence time could be significantly greater than a century and thus the surface composition might be helium rather than hydrogen (see [122] for a discussion of what the larger implied radii would mean for dense matter).

Moreover, it is not necessarily valid to assume that the entire surface radiates uniformly. Nonaxisymmetric emission could theoretically show up as detectable pulses, but if the magnetic pole is close to the rotational pole (as was suggested to explain phenomena including the lack of pulsations in most LMXBs; see [115; 114]) the pulsations could be undetectable while leading to inferred radii that are too low.

In addition, there are several puzzling aspects to the quiescent emission. For stars that have undergone several outbursts we have a decent estimate of their overall accretion rate. We can thus estimate the luminosity produced in the crust by electron capture reactions (e.g., [40]), which should be the minimum emergent luminosity. We also expect that the flux we see from the star should decline smoothly after cessation of accretion, and thus not have short timescale increases and decreases. In addition, if cooling is the only process, the spectrum should be purely thermal. All these expectations are violated in several stars. The quiescent thermal luminosity of H1905+00 is $L < 2 \times 10^{30}$ erg s^{-1}, which is significantly below standard predictions [99]. Several stars vary in intensity by a factor of a few on timescales of days to years during their decline (for a discussion see [197]). In addition, many of the field low-luminosity stars have significant, even dominant, nonthermal tails (e.g., Cen X-4; [178]).

It is possible that these discrepancies can be understood within the basic picture. For example, enhanced neutrino emission in the crust would not be observed, so this could explain the underluminous stars. Short timescale variability might be caused by the motion of obscuring matter in these binaries. Nonthermal spectral tails could be caused by coronal emission from the companion star [45; 27], magnetospheric activity, or some small residual accretion. Thus although the simple model is contradicted, plausible additions could rescue it. This nonetheless contributes an additional note of caution to radius inferences from these stars.

The second category of source for spectral modeling and radius inferences is isolated neutron stars. We will encounter these again in § 5 when we discuss cooling processes, but here we focus on what can be learned about radii. Exactly the same

principles apply as for the qLMXBs, except that these stars do not accrete (the accretion rate from the interstellar medium is negligible; see [28] for a discussion). The same questions apply for these stars as they do for qLMXBs. For example, the spectra of young isolated neutron stars (such as the Crab pulsar) have significant nonthermal components probably caused by magnetospheric emission. Distances are also often difficult to establish, and the spectra can be fit using various spectra that give significantly different answers for the radius.

A case in point is RX J1856.5–3754, which is the brightest of the eight thermally emitting isolated neutron stars discovered using ROSAT. Its spectrum is featureless and can be fitted using a Planck spectrum, a heavy element spectrum, or a spectrum appropriate for condensed matter with a thin hydrogen envelope [187]. An interesting puzzle that constrains the atmospheric model is that the best-fit Planck spectrum to the X-ray data underpredicts the optical flux by a factor of ~ 6 [42]. The distance has been estimated to be 117 ± 12 pc [207] or 161 ± 12 pc [202], although the data for the latter were re-analyzed to find a distance of 123^{+11}_{-15} pc [206]. It has been argued that this star has a radius of > 14 km, which if true would make a strong case for hard equations of state. However, better atmospheric modeling suggests a radius of 11.5 ± 1.2 km [187] assuming a distance of 120 pc, which makes the radius consistent with standard nucleonic and quark matter equations of state.

Other stars have been fit in the same manner; see for example [209; 83; 84]. Table 2 of [209] gives fitted radii for three neutron stars in globular clusters, and Table 4 of [83] gives fits for $R_\infty \equiv R(1-2GM/Rc^2)^{-1/2}$ for a number of qLMXBs and neutron stars in globulars. The uncertainties are large in many cases and thus these measurements tend not to be good discriminants between equations of state. In addition, it must be kept in mind that, as with the qLMXBs, the stars are so dim that their observed spectra cannot easily discriminate between quite different models, whether these be hydrogen atmospheres, helium atmospheres, Planck spectra, or heavy elements (see Figure 3). Finally, it must be recalled that we know of nonaccreting neutron stars that pulse in the X-rays. If the isolated neutron stars we see that do not appear to pulse simply have their magnetic axes nearly aligned with their rotational axes, then single-temperature fits are likely to be misleading. Large-area instruments or long observations such as those planned for NICER [81] or LOFT [70] would help greatly in distinguishing between models.

4.3 Modeling of waveforms

Thermonuclear bursts that display brightness oscillations, and isolated millisecond pulsars that are detectable in X-rays, have had their periodic waveforms analyzed in attempts to constrain their masses and radii. The basic principle is simple: if one makes the standard assumption that the oscillations are rotational modulations of the flux produced by a hot spot fixed on the star, then the shape of the waveform encodes information about the mass and radius. For example, a star of a given rotation frequency that has a large radius will have a higher linear surface rotational speed at

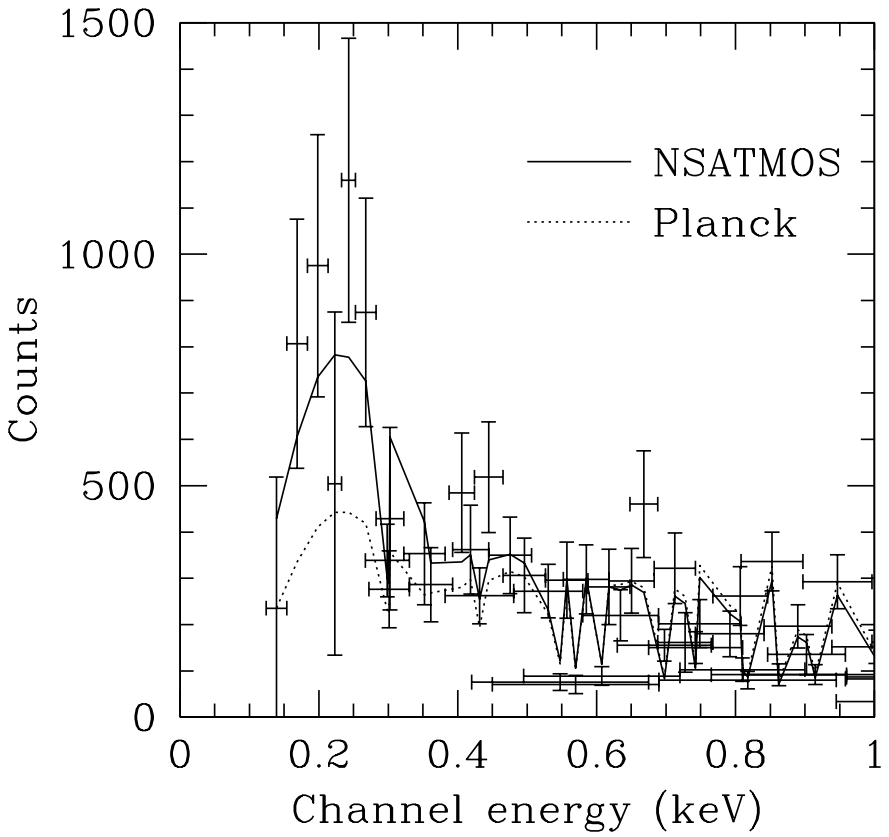

Fig. 3 XMM spectrum (error bars) and fits to a neutron star atmosphere model (solid line) and a blackbody (dotted line) for a neutron star in the globular cluster M13 (see [209]). The total chi squared for the blackbody fit is $\chi^2 = 88$ for 59 degrees of freedom, compared with $\chi^2 = 64$ in the NSATMOS model, so for the three extra parameters the difference is slightly greater than 4σ. The fitted radius of emission in the blackbody model is only ~ 3 km, which is unphysically low unless only a small portion of the polar caps is emitting. The blackbody model can thus be tentatively ruled out on physical grounds and by a goodness of fit measure. However, a Planck function with an efficiency much less than the 100% efficiency of a blackbody is viable. Note also that the differences between a nonmagnetic hydrogen atmosphere and other candidates (e.g., pure helium, heavy atmospheres, or condensed surfaces; see [49; 187]) are much less than their differences from a blackbody, and as these give significantly different inferred stellar radii, caution is essential in these inferences. Data and model kindly provided by Natalie Webb.

a given latitude than a star with a small radius. Thus the waveform will have greater asymmetries produced by Doppler effects if the star is large than if it is small. The mass to radius ratio affects the fraction of the cycle when the spot is visible; in the

Newtonian limit $R \gg GM/c^2$ exactly half the surface is visible, but for radii appropriate to neutron stars light-bending effects make more of the surface visible, and for a slowly rotating star with $R < 3.5GM/c^2$ the entire surface can be seen. More compact stars will therefore tend to produce lower amplitude waveforms. Hence in principle a waveform can be analyzed to infer the radius and mass, as well as other quantities such as the rotational latitude of the spot center, the rotational latitude of the observer, the spot angular radius (which turns out to be unimportant, as does the spot shape, as long as the spot radius is significantly less than the latitude of the spot center), and the emission pattern from the surface as seen in the spot's local rest frame.

Work by [148] initially appeared to cast doubt on this model of burst oscillations, because when they stacked data from multiple bursts from a given star they seemed to find that in some cases high energy photons arrive after low energy photons, i.e., the hard photons lag the soft photons. This is unexpected in the rotating hot spot model because as the spot rotates into view, the Doppler effect blueshifts the spectrum and thus high energies should lead low energies. However, a careful re-examination of the data for 4U 1636–536, which showed the strongest hard-lag trend in [148], showed that in fact the oscillation phase versus photon energy is entirely consistent with the rotating hot spot model [9]. Statistical fluctuations, and probably the consequences of stacking burst data, appear to have led to the opposite conclusion in [148]. Thus currently it does appear that rotating hot spots are consistent with the data on burst oscillations.

The most common assumption in such modeling is the "Schwarzschild plus Doppler" approximation (e.g., [143; 211; 150; 26]), in which the star is assumed to be spherical and the spacetime external to the star is assumed to be Schwarzschild (nonrotating), but all the special relativistic effects associated with the rotation of the surface are treated exactly. Full simulations that trace rays in the numerical spacetimes appropriate for rotating objects have demonstrated that the waveforms generated using the Schwarzschild+Doppler approximation are indistinguishable from the waveforms in the full simulation when there are $\lesssim 10^5$ total counts and the stars have radii $R < 15$ km and spin frequencies $\nu < 600$ Hz [38; 44]. The current best analyses of isolated millisecond pulsars and bursting stars yield radii that are consistent with expectations but not very constraining; [33] find that J0030+0451 has a radius > 9.4 km and J2124–3358 has a radius > 7.8 km (both at 68% confidence, and both assuming $M = 1.4\ M_\odot$), and [26] find $Rc^2/GM > 4.2$ at 90% confidence for the burster XTE J1814–338. Analyses using the "oblate Schwarzschild" approximation (in which the star is allowed to be oblate due to rotation but the spacetime is still assumed to be Schwarzschild) for SAX J1808.4–3658 [147] and XTE J1807–294 [123] are similarly unconstraining. The strongest current constraints from this method come from a recent analysis of PSR J0437–4715 assuming a hydrogen atmosphere, for which the result is $R > 11.1$ km at 3σ confidence [32].

A key assumption in the analysis of [32] is that the angular distribution of radiation from a point on the surface can be described by the pattern that emerges when the energy is deposited deep and propagates through a pure nonmagnetic hydrogen atmosphere. This could be a correct assumption, but in addition to our previous

comments that hydrogen might not be the dominant surface composition, we note that the assumption of deep deposition of energy (which for this source comes from the return current of relativistic pairs from the magnetosphere) is based on the idea that the current gives up its energy via bremsstrahlung and nothing else. Given that plasma instabilities can shorten by orders of magnitude the column depth of energy deposition (see [39] for a recent example in the context of how AGN jet energy is injected in the intergalactic medium), this might not be a safe assumption.

There are two reasons for the large confidence regions that currently arise from analyses of waveforms: (1) the total number of counts is small, and (2) there are significant degeneracies between the parameters that produce the waveform. The effects of both factors are expected to be addressed using the next generation of large-area X-ray timing satellites. As discussed by [126], if a million counts are received from the spot (comparable to the total number expected from combining several bursts observed using LOFT) and the center of the hot spot and the observer are both within 10° of the rotational equator, then M and R can both be obtained to 10% precision.

As with the other methods we discuss, a key question is the role of systematic errors: if some aspect of the real system differs from what we assume in our model fits, how badly will our inferred mass and radius be skewed? There are clearly an unlimited number of possible sources of systematic error, but an encouraging conclusion from the work done by [126] with synthetic data is that even if the assumed surface beaming pattern, spot shape, or spectrum differ significantly from the actual ones, fits using the standard model do not *simultaneously* produce (1) a statistically good fit, (2) apparently strong constraints on M and R, and (3) significant bias in M and R. Thus, at least for the systematic differences from the model explored by [126], if the fit is good and the constraints are strong, the inferred values of the mass and radius are reliable.

Valuable extra information could be obtained from the identification of atomic lines from the surfaces of rotating neutron stars. No such line has been confirmed, and indeed even if a line-like feature is seen in a spectrum it is not trivial to identify the $z = 0$ atomic transition corresponding to the line. One such identification was claimed from an analysis of stacked bursts from EXO 0748 [58], but an additional long look at the star found it in another state that had no lines at all, whether zero redshift or from the surface, and thus was unable to confirm the lines [59]. The spin frequency of this star is 552 Hz [79] rather than the originally claimed 45 Hz [205], and hence one might expect that Doppler smearing would make a sharp line undetectable (although note that [17] suggest that sharp lines would still be visible; if this result is confirmed, it means that there are better prospects for sharp lines than previously thought). If future large-area instruments are able to not only detect such features but also measure them precisely, then both the redshift from the surface and the linear speed of the surface at the spot, as well as possibly even frame-dragging effects, could be inferred [25]. This would allow many degeneracies to be broken and would lead to much more precise constraints on neutron star masses and radii (and moments of inertia from frame-dragging). Note that such measurements will only be possible from actively accreting stars, because heavy elements sink in the

atmospheres of isolated neutron stars within seconds [5]. It has also been proposed that the equivalent width of the line will allow a measurement of the surface gravity, and hence that M/R (from the redshift) and M/R^2 (from the surface gravity) can be measured independently (e.g., [51]). In principle this is also possible using a non-thermal continuum spectrum, but this would require exceptional data.

4.4 Maximum spin rate

Another method that has been suggested to constrain the radius (or more properly, the average density) is measurements of spin frequencies: a high enough spin frequency from any star would rule out the hardest equations of state. Unfortunately, no confirmed spin frequency is high enough to place significant limits on dense matter. The maximum spin frequency for a star of mass M and radius R is roughly [56]

$$\nu_{\rm max} = 1250 \ {\rm Hz} \, (M/M_\odot)^{1/2} \, (R/10 \ {\rm km})^{-3/2} \, . \tag{14}$$

This is ≈ 800 Hz for $M = 1.4 \ M_\odot$ and $R = 15$ km. In comparison, the highest frequency ever established is 716 Hz, for PSR J1748–2446ad in the globular cluster Terzan 5 [93]. Weak evidence for an 1122 Hz signal during thermonuclear bursts from XTE J1739–285 has been claimed [102] but not confirmed. Even if it were confirmed there would have to be strong evidence that this was the fundamental frequency instead of the first overtone; the overtone can be dominant, as was shown for IGR J17511-3057 [6].

Given that neutron stars could spin faster than they do, and that X-ray observations using the *Rossi* X-ray Timing Explorer are not biased against signals with $\nu > 1000$ Hz [47], why do the stars not spin faster? A conservative answer that is in agreement with all data is that magnetic torques during accretion and spinup limit the frequency. The required dipolar field strengths $\sim 10^8$ G agree with the fields inferred from the spindown of their descendants (the rotation-powered millisecond pulsars), and in particular with the adherence of those pulsars to the spin-up line [132]. Fields of this strength are also consistent with the spin behavior of stars between transient outbursts [89; 162]. Another possibility is that in many cases not enough matter has been accreted to reach maximum spin. An exciting longshot that has received much attention due to the rapid improvements in ground-based gravitational wave detectors is that nonaxisymmetries in neutron stars, e.g., Rossby waves [7; 53; 34] (see [88; 130] for recent observational constraints) or perhaps accretion-induced lumpiness in the stars [196], might counteract accretion spinup via emission of gravitational radiation. One way to test this hypothesis is to observe systems that have had multiple transient episodes, because the spindown between active phases could indicate whether gravitational radiation (which would depend only on the long-term average accretion rate rather than the instantaneous rate) emits angular momentum at the required rate. Two such systems (SAX J1808–3658 and IGR J00291+5934) have been observed with the required precision. In both cases

there is no evidence that gravitational radiation induced spindown is occurring, but within the observational uncertainties there is room for contributions at the tens of percent level [87; 161]. Whatever the reason for the spin ceiling, at this stage there are no known neutron stars with spin frequencies high enough to rule out any plausible equation of state.

4.5 Kilohertz QPOs

Kilohertz quasi-periodic brightness oscillations (kHz QPOs) from accreting neutron stars have been proposed to constrain the masses and radii of the stars. The basic phenomenology of kHz QPOs is that there are commonly two relatively narrow ($Q \equiv \nu/\mathrm{FWHM} \sim 20-200$) QPOs that appear in the power density spectra of more than 25 neutron star low-mass X-ray binaries. Both frequencies vary by hundreds of Hertz between and during observations. The higher-frequency of the two often reaches $\nu > 1000$ Hz, and the lower-frequency peak (which is often the sharper one, and also commonly has a larger fractional root mean square amplitude) has a frequency less than that of the upper peak by a characteristic but not exactly constant amount that may be related to the spin frequency of the star (but see [137] for a dissenting opinion).

Most, but not all, modelers identify the upper peak frequency with an orbital frequency at some characteristic radius around the star. If this is true, it means that the star must fit inside that radius, as must the radius of the innermost stable circular orbit (ISCO) predicted by general relativity; the latter condition follows because matter inside the ISCO will fall rapidly towards the star and thus prevent it from forming high quality factor oscillations. As derived by [145], for a neutron star with a dimensionless rotation parameter $j \equiv cJ/GM^2$ these conditions limit the mass and radius to $M_{\mathrm{max}} = 2.2\,M_{\odot}(1+0.75j)(1000\ \mathrm{Hz}/\nu_{\mathrm{QPO}})$ and $R_{\mathrm{max}} = 19.5\ \mathrm{km}(1+0.2j)(1000\ \mathrm{Hz}/\nu_{\mathrm{QPO}})$ for an upper peak frequency ν_{QPO}. The highest confirmed QPO frequencies are all less than 1300 Hz (see, e.g., [35] for a discussion of the 1330 Hz QPO once suggested for 4U 0614+09), so at this stage the constraints are not restrictive. If broad iron lines from the inner disk are discovered simultaneously with kilohertz QPOs, this will provide another measure of the mass because the line breadth gives $\sqrt{M/r}$ whereas the QPO frequency gives $\sqrt{M/r^3}$ at the orbital radius r (see [43] for current data and [24] for future prospects; note that the Kerr spacetime is not an adequate approximation for sufficiently rapidly rotating neutron stars [144]). Similarly, if reverberation mapping can establish an absolute time scale for the system, this might yield masses and radii [12].

If the orbital frequency of the ISCO is established for a star, then the mass of the star is known to within a small uncertainty related to the star's dimensionless angular momentum parameter. After doubt was cast on initial claims of ISCO signatures [218] because of the complex relation between count rate and QPO frequency in these stars [138], recent analysis of the RXTE database has suggested that in many stars the predicted sharp drop in quality factor and gradual drop in amplitude [145]

are seen at a frequency that is consistent across a wide range in count rate and X-ray colors [13; 14; 15; 16]. The independence of this behavior from proxies of mass accretion rate such as count rate and colors led these authors to suggest that a spacetime marker such as the ISCO was the most likely reason for the observed phenomena. If so, this represents a confirmation of a key prediction of strong-gravity general relativity (the ISCO), and implies masses greater than 2.0 $M_\odot$ for some neutron stars, which would be highly constraining on equations of state.

Such important implications demand careful examination. For example, [136] notes that the maximum quality factor achieved by neutron star LMXBs, versus their average luminosity, has a shape similar to the quality factor versus radius in individual stars, and uses this to conclude that other factors operate and that the drop in quality factor might not be caused by approach to the ISCO. Indeed, other factors do influence the quality factor; for example, the high-luminosity stars plotted by [136] have geometrically thick disks that cannot produce high-Q oscillations. This is thus not directly relevant to the arguments made by [13; 14; 15; 16] because the stars they examined are all low-luminosity, and hence the results of [136] do not address whether the ISCO causes the behavior observed in those stars. Nonetheless, the complex phenomenology of kHz QPOs and the lack of first-principles numerical simulations that display them means that claims that the ISCO has been detected must be treated with care.

4.6 Other methods to determine the radius and future prospects

There are two other noteworthy ways to measure the radius that have been suggested with particular applications to the double pulsar J0737. The first involves the binding energy of the lower-mass Pulsar B in that system. Based on an idea originally proposed by [151], [165] suggested that this neutron star formed via an electron-capture supernova (in which electron captures onto Mg and then Ne in a core cause a loss of pressure support) rather than the usually considered collapse of an iron core when it goes above the Chandrasekhar mass. As this electron capture happens at a very specific central density of 4.5×10^9 g cm^{-3} that corresponds to a well-defined baryonic mass of $M_{\rm bary}=1.366-1.375\,M_\odot$ [165], if one could identify this baryonic mass with the gravitational mass $M_{\rm grav}=1.2489\pm0.0007\,M_\odot$ of Pulsar B then one would have an extremely precise constraint that would suggest a fairly hard equation of state. However, there is an unknown amount of fallback after the initial collapse, so the electron capture scenario only suggests that $M_{\rm bary}(M_{\rm grav}=1.2489\,M_\odot)>1.366-1.375\,M_\odot$. This allows a wide variety of equations of state.

The second method stems from the observation that spin-orbit coupling, which is dominated in this system by the 23 ms period Pulsar A instead of the 2.8 s period Pulsar B, leads to precession of the orbital plane and additional pericenter precession [11; 61; 129; 121; 106]. Orbital plane precession will be difficult to measure, but the required precision for the extra pericenter precession could be reached in the

next few years [121]. Such a measurement would effectively determine the moment of inertia I of Pulsar A (potentially to 10%; [121]), and given that $I \sim MR^2$ and M is known well, this would amount to a $\sim 5\%$ measurement of the radius. It is unclear whether this will be reachable in practice, because of the confusing effect of the unknown acceleration of the center of mass of the binary within the Galactic potential [106].

In general, the methods discussed in this section have uncertainties that are dominated by systematics. As a result, future progress depends on both better observations and better models. For example, there is a recent set of magnetohydrodynamic simulations that aim to reproduce kHz QPO phenomenology in accreting weakly magnetic neutron stars [176; 175; 107; 173; 127; 128; 174; 108; 31]. These simulations may ultimately result in solid understanding of kHz QPOs that could be used to interpret observations. The simulations are extremely challenging, however, and may take many years to get to the point of full reliability. Some of the apparently disparate constraints may eventually be coupled through the recently discovered "I-Love-Q" relations between the moment of inertia I, Love number, and quadrupole moment Q [214], although the important issues of systematics must be solved first.

5 Cooling of Neutron Stars

As noted in § 2, cooling processes are sensitive to different aspects of the equation of state than are the maximum mass and the mass-radius relation. This in principle means that observations of cooling neutron stars can give us a complementary tool with which to constrain the properties of dense matter. In fact, current data are broadly consistent with the dense matter in neutron stars not having significant contributions from exotic phases (modulo some complications we shall discuss), but unfortunately as we will see this is a very blunt tool and there is plenty of room for exotic matter.

X-rays from cooling neutron stars were originally proposed in the mid-1960s [55] as one of the few ways that these stars could be detected. In this section we will focus on cooling theory and observations that bear on the matter at the cores of neutron stars. We will thus not discuss, e.g., the cooling of transiently accreting neutron stars (see [215; 157] for recent reviews) that return to quiescence after a years-long outburst has raised the crust out of thermal equilibrium with the core, because their cooling curves depend primarily on processes in the crust.

Broadly speaking, after a neutron star forms in a supernova (where at birth its temperature is roughly the virial temperature $T_{\rm vir} \sim GMm_n/(Rk) \sim 10^{12}$ K), the star goes through a phase of duration $\sim 10^{4-6}$ yr in which its cooling is dominated by neutrino losses from the core. After this point the star cools mainly by photon luminosity from the surface, where the energy from the core is transported conductively until the density is low enough that radiative processes take over (this typically occurs in the outer crust). The temperature of a neutron star at a given age therefore depends strongly on how long neutrino emission dominates. The temperature tool is

blunt because there are many processes that can enhance neutrino production, and many processes that can suppress it, and thus mere measurement of the temperature with age of neutron stars would not allow us to distinguish easily between the multiple candidate effects.

5.1 The URCA processes

To start, we note that as the star cools down from its high-temperature birth the processes $p+e^- \rightarrow n+\nu_e$ and $n \rightarrow p+e^-+\overline{\nu}_e$ can produce neutrinos efficiently. In this context these are known as the URCA processes, named thus by George Gamow after the Urca casino in Rio de Janeiro because the URCA processes are a perfect sink for energy just as the casino is a perfect sink for money! Phase space considerations indicate that the URCA emissivity (energy per volume per time) scales as T^6.

As the temperature cools below the Fermi temperature, however, we can see that these processes become impossible unless the proton to neutron ratio is sufficiently high. The derivation of the critical ratio is similar to what we presented in § 2: the momenta of the particles, which are dominated by Fermi momenta, must satisfy the triangle inequality $p_n \leq p_p + p_e$. The Fermi momenta of all three particles are determined by their respective number densities, so this means $n_n^{1/3} \leq n_p^{1/3} + n_e^{1/3}$. Charge neutrality means $n_e = n_p$, so $n_n^{1/3} \leq 2n_p^{1/3}$ and thus the criterion for the URCA process to be possible is $n_n \leq 8n_p$. This is on the low side for many traditional equations of state but can be achieved in some cases at high density. Note that if muons are also present (these are higher-mass analogs to electrons with the same electric charge), and thus electrons have a number density $n_e = xn_p$ with $x \leq 1$, the criterion becomes $n_n \leq (1+x^{1/3})^3 n_p$, so even higher proton fractions would be required.

If the URCA process is suppressed, bystander particles can soak up the extra momentum, e.g., $n+n \rightarrow n+p+e^-+\overline{\nu}_e$. This is usually called the modified URCA process to distinguish it from the direct URCA (sometimes DURCA) processes described above. Given that the neutrons are degenerate, only a fraction T/T_F of them can interact. Thus the modified URCA process is suppressed by a factor $(T/T_F)^2$ (one factor is for the initial neutron and one is for the final) compared to the direct URCA process. Given that in a neutron star core $T_F \sim 10^{12}$ K and T can be $\sim 10^9$ K, the suppression factor can easily be a million.

The huge difference between the direct and modified URCA rates means that if enough protons are present, or if there are any other channels for neutrino production, then cooling can be enhanced dramatically. We now consider such channels.

5.2 Additional neutrino production channels and suppression

As described in the lucid review of [157], hyperons can produce neutrinos via, e.g., $\Sigma^- \to \Lambda + e^- + \bar{\nu}_e$, $\Lambda + e^- \to \Sigma^- + \nu_e$, and processes that involve both hyperons and nucleons. If condensates form (the leading candidates are of pions or kaons) then the condensate acts as an effectively infinite reservoir of momentum. This produces channels such as $n + \langle \pi^- \rangle \to n + e^- + \bar{\nu}_e$ and $n + \langle K^- \rangle \to n + e^- + \bar{\nu}_e$, where the angle brackets indicate the condensate. The kaon process involves a strangeness change and is thus less efficient than the pion process, modulo effects related to the medium [157]. If deconfined quarks are a significant degree of freedom then other direct URCA-like processes can emerge, such as $u + e^- \to d + \nu_e$ and its inverse (e^+ could be present in negatively charged quark matter, but the processes are the same), and $u + e^- \to s + \nu_e$ and its inverse (suppressed by an order of magnitude because of the strangeness change). All of these processes are orders of magnitude more efficient than modified URCA, and all scale as T^6.

A separate channel has the interesting property that it can both increase and suppress cooling, depending on the details. This is the transition to a superfluid state. This transition occurs via Cooper pairing of the neutrons, and the immediate effect is the emission of a neutrino-antineutrino pair: $n + n \to [nn] + \nu + \bar{\nu}$. Given that one fewer effective particle is involved than in modified URCA the emissivity scales as T^7 instead of T^8, so at $T \sim 10^9$ K the emissivity of Cooper pairing can be comparable to or greater than modified URCA. As the shell where the temperature is less than the superfluid critical temperature moves inwards, this can therefore enhance neutrino emission.

In the long term, however, the pairing produces an energy gap $\Delta \sim kT_c$ (where T_c is the superfluid critical temperature) at the Fermi surface that suppresses processes by a factor of order $e^{-\Delta/kT}$ for $T \ll T_c$, modulo details of the phase space and the temperature dependence of Δ. The suppression can thus be extremely dramatic. It occurs for both the neutrino emissivity and for the specific heat (with different factors). See, e.g., Figure 5 of [157] for plots of some of the suppression factors (called control functions there). The critical temperature and energy gap are extremely difficult to calculate from first principles but most estimates suggest $\Delta \sim 1$ MeV, which corresponds to $T \sim 10^{10}$ K and is thus enough larger than core temperatures to make a significant difference.

Cooper pairing can also occur in deconfined quark matter. In that context it is much more complicated than in ordinary matter because quarks have different colors, flavors, and masses. Multiple types of condensation are therefore possible. The color gap is estimated to be $\sim 50 - 100$ MeV [157], which is huge compared to internal temperatures and is thus potentially quite important.

There are also neutrino emission processes in the crust of the star, such as plasmon decay and neutrino pair bremsstrahlung from electron-ion and electron-electron interactions. These could contribute for middle-aged stars, when the core processes are suppressed by the superfluidity gap and the crust is warm enough to produce neutrinos.

5.3 Photon luminosity and the minimal cooling model

When neutrino emission has tapered off, further cooling of the star is controlled by conductive transport in the dense layers of the star (where electrons are degenerate and thus have large mean free paths) and by radiative transport nearer the surface. There is a minimum in the overall efficiency of energy transport at the "sensitivity layer" where conduction hands off to radiation (where electrons are only partially degenerate). This thus acts as a bottleneck and largely determines the overall cooling rate; the density at the sensitivity layer increases with increasing temperature. For temperatures in the observed range $\sim 10^{5-6}$ K the sensitivity layer is at a density $< 10^9$ g cm^{-3}, where pycnonuclear fusion is not guaranteed to convert light elements to heavy ones. The electron thermal conductivity in liquid ions depends on their charge Z as $\sim 1/Z$ [157], so differences in the composition of the upper layers (due, e.g., to different fall-back after core collapse) could have an influence on the thermal evolution of neutron stars.

Conduction dominates at high enough densities that magnetic fields are likely to be unimportant: at typical densities $\rho \gtrsim 10^6$ g cm^{-3} the Fermi energy is $E_F \gtrsim m_e c^2$, implying that the magnetic field needs to be $B \gtrsim B_c = m_e c^3/(\hbar e) = 4.414 \times 10^{13}$ G to have a significant influence. However, more moderate magnetic fields can affect radiative transport near the surface. More specifically, suppression of electron motion across field lines yields anisotropic conduction. This can produce strong anisotropies in the emergent radiation, but the overall effect on cooling is relatively small [157]. Ultimately, the radiation emerges with some spectrum and an effective temperature $T_{\rm eff}$ that can be defined as

$$T_{\rm eff}^4 \equiv \frac{1}{4\pi} \int \int T_s^4(\theta,\phi) \sin\theta d\theta \, d\phi \, . \tag{15}$$

Here, the local effective temperature $T_s(\theta,\phi)$ at each location (θ,ϕ) on the surface is defined via $\sigma_{\rm SB} T_s^4(\theta,\phi) = F(\theta,\phi)$ where F is the emergent photon flux and these quantities are appropriately redshifted. If the emergent spectrum is close to a blackbody then one can estimate the temperature without knowing the distance to the star (see § 4), but as we discussed earlier atmospheric effects cause the spectrum to deviate from a blackbody form, which complicates inferences.

With this physics in place one can construct a surface temperature versus age curve by including a specific choice for the uncertain core processes as well as choosing the composition of the surface layers. A particularly useful choice is the "minimal cooling model" (see [158] for a recent treatment), in which one assumes no exotic components or direct URCA but does include Cooper pairing, crustal bremsstrahlung, and all relevant photon processes. This represents the smallest amount of cooling that is realistic. As a result, if there is evidence that at least some neutron stars are significantly cooler than they are predicted to be in this model, that might suggest exotic components (although it does not work the other way around; conformity with minimal cooling might mean the suppression effects are important). To see how this cooling model fares we now turn to observations.

5.4 Observations and systematic errors

Before discussing the observations we must issue a series of caveats. There are many reasons why it is difficult to generate reliable points on a temperature-age curve, including the interpretation of the spectrum, other possible heating sources, and challenges with age estimation. We now discuss these in order before finally evaluating the best current data on cooling neutron stars.

A neutron star with a surface effective temperature of 10^6 K and a radius of 10 km has a luminosity of $L \sim 10^{32}$ erg s^{-1}, which at a distance of 3 kpc gives a detector flux of $F \approx 7 \times 10^{-13}$ erg cm^{-2} s^{-1} and corresponds to ~ 2 counts per second for a 1000 cm^2 detector. It is therefore possible to get a reasonable number of photons over a long observation, although the thermal peak of $\sim 0.2\ \mathrm{keV}(T/10^6\ \mathrm{K})$ is strongly susceptible to interstellar absorption.

There are also complications with the atmospheric model, as we discussed when we examined radius estimates for cooling neutron stars. For example, compared to a blackbody with the same effective temperature, an unmagnetized hydrogen atmosphere has a strong excess at higher energies when absorption dominates the opacity, because these opacities scale as ν^{-3} (e.g., [179]). Magnetized hydrogen has less of an excess because strong fields increase the binding energy of atoms (e.g., Problem 3 in §112 of [116]), and heavier elements also have more bound electrons and thus less of an opacity deficit at high energies compared to lighter elements [171; 146; 140; 168]. Observational support for the diffusive burning of hydrogen or helium [49; 50] may have been obtained from the evidence that the atmosphere of Cas A is dominated by carbon [95]. As a result, unless there is a clear statistical preference for one atmospheric model versus another (which is not currently the case for any star), the temperature will be uncertain.

We must also be cautious because in addition to simple cooling there are various heat sources that could contribute. These include magnetic dissipation (likely only important for highly magnetic neutron stars) and magnetospheric emission. The latter is likely to produce a nonthermal spectrum, which is indeed seen in some stars. One could argue with some justice that if we are looking for cases where the temperature is *less* than predicted by the minimal cooling model, other heat sources will only mean that such evidence is even stronger. The tricky part comes when one subtracts off nonthermal components to estimate the underlying thermal emission; if the other components were oversubtracted this would lead to an underestimate of the cooling temperature.

The final caveat relates to the age. If the star was born with a much more rapid spin than it has now and it has slowed down exclusively by magnetic dipole radiation then its current age is $P/(2\dot{P})$, where P is the current spin period and $\dot{P}$ is the current spin derivative. In some cases this age estimate can be checked using a kinematic age, either from a supernova remnant or from the angular distance above the Galactic plane (where massive stars are born) divided by the angular proper motion away from the plane. Unfortunately there is often a discrepancy between these estimates of a factor of three or more, so all of these numbers must be treated with caution.

With the preceding in mind, Figure 8 in [158] shows the comparison between the minimal cooling model (with light or heavy element envelopes) and the data. Within the significant uncertainties we note that all of the data are consistent with the minimal cooling model, although there is some evidence that variation in the envelope composition is needed to explain the data. As [156] note, however, there is a significant selection effect at work: if there are stars that have cooled rapidly, they are obviously more difficult to see. It is thus possible that using our current satellites we can only observe comparatively hot stars.

Recently it was suggested that the neutron star in the supernova remnant Cas A has cooled very rapidly over the past decade or so [95]. Further observational analyses, especially taking into account the complexity of the surrounding supernova remnant emission [68] and the possibility of changes in the calibration, emitting region size, or absorbing column [166] have made it much less clear that there actually is anomalously fast cooling. If the evidence strengthens for such cooling, it has potentially exciting implications for the physics of the interior of this neutron star, with the leading idea being Cooper pair creation in the superfluid [183; 159]. One-pion exchange and polarization effects could also play a role [30].

5.5 Current status and future prospects

Currently there is no evidence that exotic components are *necessary*, although given the large uncertainties in data they could certainly be *accommodated*. The possible lack of exotic components is consistent with the tentative evidence presented in § 4 that some neutron stars have masses $\gtrsim 2.0\ M_\odot$, and could mean that nucleonic degrees of freedom dominate the internal structure of neutron stars. However, the data are not clear.

To improve the observational situation it will be necessary to have much larger-area future X-ray observatories, such as the planned ATHENA+ [149]. The resulting high-signal observations would play two important roles: (1) they would reduce the bias against rapidly cooled stars, and would thus possibly reveal evidence for exotic components, and (2) they would allow us to distinguish empirically between different candidate atmospheric spectra (nonmagnetic hydrogen or helium, magnetic atmospheres, and even the straw man blackbody spectrum), and thus have greater confidence in the inferred temperatures. It will be more challenging to come up with much more precise and accurate ages, but it could be that future radio arrays such as the Square Kilometer Array will allow us to determine the proper motion and kinetic ages more accurately.

6 Gravitational Waves from Coalescing Binaries

In the next few years it is expected that the worldwide gravitational wave detector network will achieve sufficient sensitivity to detect $\sim 0.4-400$ NS-NS mergers per year, and an uncertain number of NS-BH coalescences (see [2] for a recent discussion of the predicted rates and their substantial uncertainties). In this section we summarize what can be learned from such observations. It has also been proposed that observation of neutron star oscillation modes stimulated by mergers or (at much lower amplitude) glitches would yield important information about the stars (see, e.g., [200; 52; 18; 54; 66]); this is true, but the amplitudes are likely to be significantly below the amplitudes of the coalescence signal, so we will not focus on oscillations here.

In brief, for a binary of masses m_1 and m_2 and thus total mass $M = m_1 + m_2$ and symmetric mass ratio $\eta = m_1 m_2/M^2$ (note that $\eta \leq 0.25$, with the maximum occurring for $m_1 = m_2$), the combination $\eta M^{5/3}$ will be determined with high precision and could lead to significant constraints if a high enough mass binary is detected. The individual masses and the average density of the neutron stars will be more challenging to measure, but they seem within reach for the strongest events.

In more detail, we note that to lowest order gravitational radiation changes the binary orbital frequency at a rate (see [163] for the rate of change of the semimajor axis)

$$\frac{df}{dt} = \frac{96}{5}(4\pi^2)^{4/3} G^{5/3} \eta M^{5/3} f^{11/3} c^{-5} (1-e^2)^{-7/2} (1+73e^2/24+37e^4/96)\,. \quad (16)$$

Now consider a NS-NS binary. When the orbital separation is much greater than the radii of the neutron stars, the inspiral of the binary proceeds almost as it would if the stars were point masses. From equation 16 we see that the mass combination $M_{\rm ch}^{5/3} \equiv \eta M^{5/3}$ (where $M_{\rm ch}$ is called the "chirp mass") determines the frequency and amplitude evolution. It can thus be measured with precisions better than 0.1% in many cases [199]. Even with no additional information we can obtain a strong lower limit to the total mass M by setting $\eta = 0.25$, and thus can obtain a strong lower limit $M/2$ to the greater of the two masses. It could be that if tens to hundreds of NS-NS mergers are observed per year, and if these can be distinguished clearly from NS-BH and BH-BH mergers, then a small number of them will have $M > 4.0\ M_\odot$ and thus it will be possible to establish rigorously that $M_{\rm max} > 2.0\ M_\odot$.

We might not be this lucky. If the NS-NS detection rates are as low as $\sim 1\ {\rm yr}^{-1}$ then high-mass binaries might not be sampled. If the rate is tens per year but the chirp masses do not imply a high minimum mass it could be that the upper limit to neutron star masses is close to the $\sim 2\ M_\odot$ that we have already established from electromagnetic observations, but it could also be that there is essentially only one way to form NS-NS systems and thus that those systems will tend to have similar chirp masses.

In these cases more information is needed. When the inspiral is followed to higher post-Newtonian order the additional terms, which involve tidal effects, have

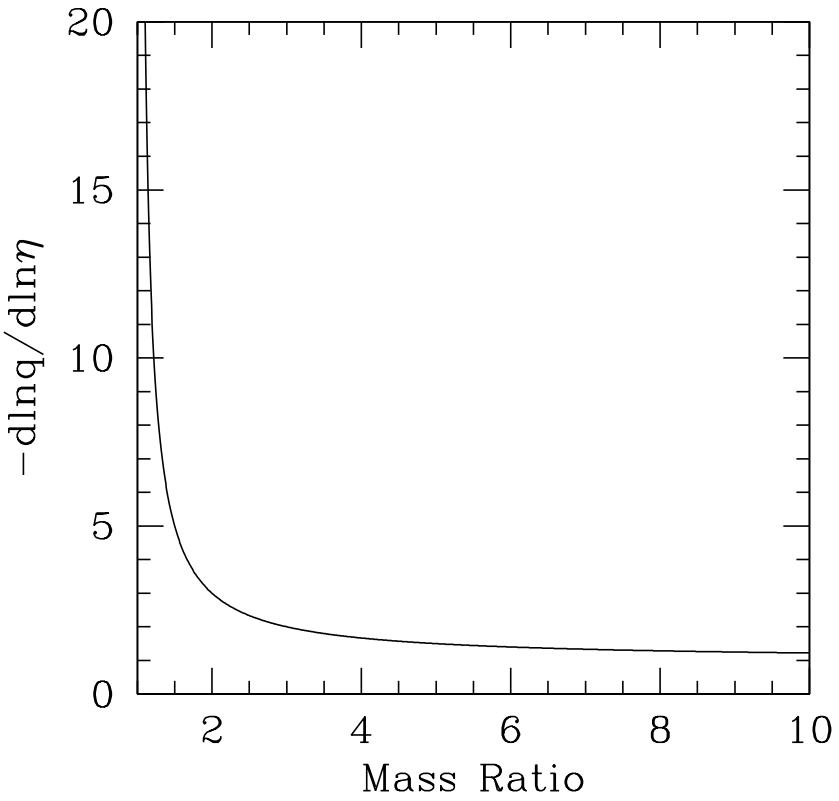

Fig. 4 Logarithmic derivative of the mass ratio $q \equiv m_1/m_2 \geq 1$ with respect to the symmetric mass ratio η. For double neutron star binaries, in which $q \sim 1$, even a small error in η leads to significant uncertainty in q. As a result, gravitational waves from double neutron star systems are not ideal for precise mass measurements of individual neutron stars.

different dependences on η and M than does the lowest-order expression, so this can be used to break the degeneracy and infer the two masses separately. For systems in which the two masses are comparable (as in a NS-NS system) this requires very high precision measurements of η. Note, for instance, that whereas $\eta = 0.25$ implies a 1:1 mass ratio, $\eta = 0.24$ implies 1.5:1. Figure 4 shows that for nearly equal masses a very small fractional error in η can still imply a large fractional error in the mass ratio $q \equiv m_1/m_2 \geq 1$. The sensitivity is naturally less away from the maximum, which might lead one to suppose that NS-BH binaries, which are asymmetric in mass, would provide greater prospects for NS mass measurements. For example, suppose that $M_{\rm ch} = 2.994\ M_\odot$ is measured with effectively zero uncertainty, and

that η is constrained to be between 0.1 and 0.11. Then the lighter component of the binary has a mass between 1.34 $M_\odot$ and 1.42 $M_\odot$ and is thus well known despite the significant fractional uncertainty in η.

The tradeoff is that black holes may typically have large enough masses that neutron stars spiral into them without significant tidal effects [141], although higher harmonics can still be important and as partial compensation they will appear at frequencies of greater sensitivity in ground-based detectors than will the corresponding harmonics in NS-NS systems. In addition black holes, unlike the neutron stars in NS-NS binaries, may well have large enough spins to affect the last part of the inspiral and thus compromise parameter estimation due to the greater complexity of the waveforms. No pulsar in a NS-NS binary has a spin period shorter than 23 ms [186], so the spin parameters of these neutron stars are $j \equiv cJ/GM^2 \lesssim 0.02$. In contrast, although inferences of the spins of stellar-mass black holes are not yet fully vetted, there is growing evidence that many of them have spin parameters of several tenths, with some possibly approaching the black hole maximum $j = 1$ [139; 133]. The likely evolutionary difference is that in the supernova that creates a neutron star or black hole, much greater amounts of mass fall back to create a black hole than a neutron star, and this mass will come from significant radii that thus carry considerable angular momentum. Accretion from a binary subsequent to the production of a black hole has little effect on either the mass or the angular momentum of the hole (see, e.g., [103]). Neutron stars in the high-mass X-ray binaries that could create a double neutron star pair accrete little mass in the active phase and, empirically, seem to have relatively strong magnetic fields, so accretion does not spin them up to high rotation rates.

These statements are not absolute. It could be that there are slowly-spinning black holes in BH-NS binaries, or rapidly spinning neutron stars in NS-NS binaries (especially if they are produced dynamically in globular clusters). However, the expectation at this time is that until tidal effects become important NS-NS waveforms will be easier to interpret than those from BH-NS coalescences.

This leads us to what those tidal effects might tell us about neutron stars. At large separations compared to the neutron star radii, nonlinear mode couplings due to tides will not affect the inspiral phase significantly [204]. Most of the information that can be obtained from tidal phase deviations from point-mass inspiral exists at high frequencies [94], and recent comparisons of analytical theory with numerical simulations suggest that with some calibration the theory does extremely well [60; 21; 71; 97; 111]. An explicit comparison of the expected signals from piecewise-polytropic equations of state suggests that a difference of only 1.3 km in radius could be distinguished for NS-NS systems out to 300 Mpc with optimal direction and binary orientation (this corresponds roughly to a direction- and orientation-averaged distance of 140 Mpc) given a full hybrid post-Newtonian plus numerical relativity waveform [170]. See Figure 5 for an indication of the different frequencies of tidal disruptions implied by two candidate equations of state.

Inspirals of neutron stars into black holes have not yet been examined using as much care with respect to phase deviations. Recent work suggests that although if the mass ratio is as high as 6:1 a NS-BH coalescence will be indistinguishable from

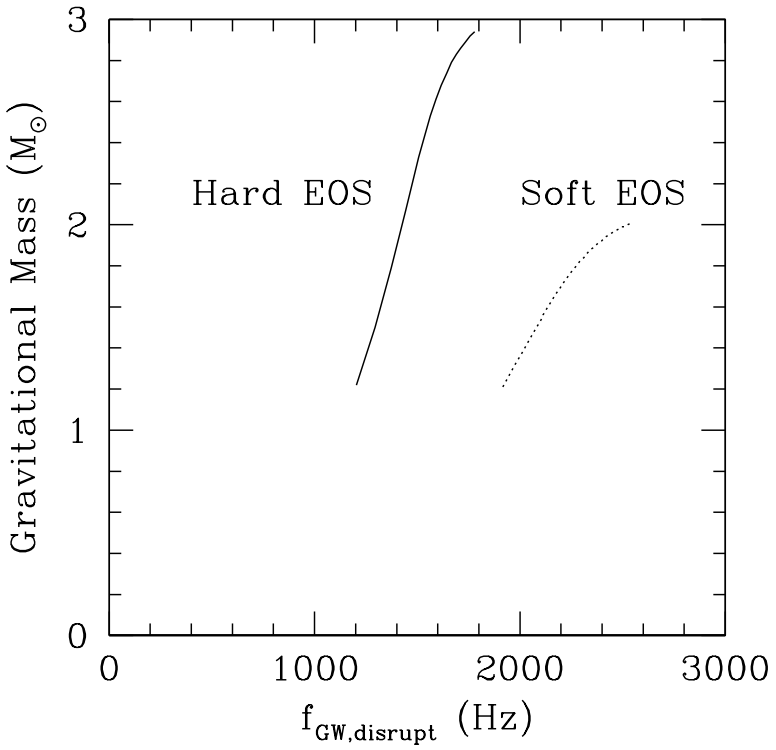

Fig. 5 Gravitational wave frequency at the point of tidal disruption as a function of neutron star mass. The solid and dotted lines refer, respectively, to the hard and soft equations of state from [91]. In both cases we assume that the companion is a neutron star of equal mass. Tidal effects will affect the phasing of the inspiral below $f_{\rm GW,disrupt}$, but the effects fall off rapidly with decreasing frequency. Good sensitivity at high frequencies is essential for these effects to be detected.

a BH-BH coalescence with the same masses [72], if the mass ratio is as small as 2:1 or 3:1, single events at a distance of 100 Mpc could reveal the neutron star radius to within 10–50% [110; 111], depending on details. This is a case in which a combination of gravitational wave and electromagnetic observations, along with simulations, would work very well: the gravitational wave observation identifies the masses of the black hole and neutron star and the spin of the black hole, and the electromagnetic observation plus simulations derives information about the remaining mass of the disk (particularly if the recent promising observations results related to kilonovae hold up; see [20; 193]). Simulations are still very much in their infancy, but this is a promising avenue to pursue. It has also been noted that the precision of constraints will be improved significantly by combining the analyses of > 10 bursts, if systematic errors are under control [64], and that observations with

the planned third-generation gravitational wave detector the Einstein Telescope will improve precision by an order of magnitude [198].

In summary, observations of gravitational waves from compact object coalescences will yield promising new constraints on the properties of neutron stars. This will occur because of new mass measurements and radius constraints. Most of the information exists at high frequencies, so in order to maximize this information it may be necessary to explore techniques beyond the second generation of detectors, such as squeezing of light [1].

7 Summary

Significant progress has been made in the last decade on mass estimates of neutron stars. The maximum mass is $\gtrsim 2\ M_{\odot}$, which along with the lack of evidence of rapid cooling suggests that non-nucleonic degrees of freedom appear unnecessary to explain current data. There is, however, considerable freedom that would allow exotic phases. The main limitation of existing observations is that radius estimates are shrouded in systematic errors. No current method is both precise and reliable enough to pose significant constraints on the structure of neutron stars. This is unfortunate, because good radii would do more than any other single measurement to inform us about the matter in the cores of neutron stars [118].

Where, then, do we stand? In the near future it is plausible that our understanding of thermonuclear X-ray bursts, accreting neutron stars, or the emission from cooling neutron stars may evolve to the point that the complex phenomena associated with them can be interpreted with confidence, and reliable radii and masses will emerge. In principle the needed data have already been collected, but our evolving understanding that, e.g., bursts do not settle quickly to a constant area of emission and that cooling neutron stars display nonthermal emission has led to caution. At the same time, numerical simulations are improving rapidly in sophistication. It is possible, although far from guaranteed, that within a few years magnetohydrodynamic simulations of accretion disks or bursting atmospheres will yield results that are close enough to what is observed that our understanding will solidify and radius measurements will become a powerful tool for constraining the state of matter in the cores of neutron stars.

If ground-based gravitational wave facilities make detections as expected within five years, then as we discussed in the previous section this will open up a new way to measure masses and radii, with systematic errors that are at a minimum different from those that bedevil current attempts, and more optimistically might be less significant than statistical uncertainties. However, most of the information resides at high frequencies where, at least for standard configurations, second-generation detectors will be insensitive enough that it may require a rare high-signal event to derive restrictive constraints. A third-generation detector such as the Einstein Telescope should be able to obtain all the required information, and even before such

detectors exist it may be possible to use configurations optimized for high frequencies or 2.5 generation technology such as squeezed light to obtain the information.

Electromagnetic observatories are also improving, and some of the old reliable methods may improve our understanding substantially. For example, the Jansky Very Large Array or (in roughly a decade) the Square Kilometer Array might have enough sensitivity, bandwidth, and computer power to detect a much larger population of double neutron star binaries, among which we might by chance have some with stars of $M > 2.0\ M_\odot$. Even without such serendipitous discoveries, the mere accumulation of time and data on NS-WD binaries in globular clusters seems likely to yield high-mass objects that will provide firm lower limits to the maximum mass that are much stronger than currently exist. As we have discussed, many other improvements are expected using the large area and excellent spectral resolution of ATHENA+ [149], and the high area and timing resolution of NICER [81] and LOFT [70]. This is especially true of radius estimates from fits to X-ray waveforms.

Overall, although we expect that eventually radius measurements will play a major role, in the next several years it appears that mass measurements of neutron stars in binaries will continue to dominate the discussion of the cold high-density equation of state. The expected improvements in data and models will allow us to provide nuclear physicists with more certain constraints, and we await the theoretical developments that result.

Acknowledgements This work was supported in part by NSF grant AST0708424, by NASA ATP grants NNX08AH29G and NNX12AG29G, and by grant number 230349 from the Simons Foundation. We appreciate helpful suggestions from Didier Barret, Paulo Bedaque, Sudip Bhattacharyya, David Blaschke, Tom Cohen, Peter Jonker, Fred Lamb, Jim Lattimer, Ilya Mandel, Dany Page, Bettina Posselt, Scott Ransom, Ingrid Stairs, and Natalie Webb.

References

[1] Aasi, J., Abadie, J., Abbott, B.P., Abbott, R., Abbott, T.D., Abernathy, M.R., Adams, C., Adams, T., Addesso, P., Adhikari, R.X., et al.: Enhanced sensitivity of the LIGO gravitational wave detector by using squeezed states of light. Nature Photonics **7**, 613–619 (2013)

[2] Abadie, J., Abbott, B.P., Abbott, R., Abernathy, M., Accadia, T., Acernese, F., Adams, C., Adhikari, R., Ajith, P., Allen, B., et al.: TOPICAL REVIEW: Predictions for the rates of compact binary coalescences observable by ground-based gravitational-wave detectors. Classical and Quantum Gravity **27**(17), 173001 (2010)

[3] Abrahamyan, S.e.a.: Measurement of the Neutron Radius of Pb208 through Parity Violation in Electron Scattering. Physical Review Letters **108**(11), 112502 (2012)

[4] Akmal, A., Pandharipande, V.R., Ravenhall, D.G.: Equation of state of nucleon matter and neutron star structure. Phys. Rev. C **58**, 1804–1828 (1998)

[5] Alcock, C., Illarionov, A.: The surface chemistry of stars. I - Diffusion of heavy ions in white dwarf envelopes. II - Fractionated accretion of interstellar matter. ApJ **235**, 534–553 (1980)
[6] Altamirano, D., Watts, A., Linares, M., Markwardt, C.B., Strohmayer, T., Patruno, A.: Type I X-ray bursts and burst oscillations in the accreting millisecond X-ray pulsar IGR J17511-3057. ArXiv e-prints (2010)
[7] Andersson, N., Kokkotas, K., Schutz, B.F.: Gravitational Radiation Limit on the Spin of Young Neutron Stars. ApJ **510**, 846–853 (1999)
[8] Antoniadis, J., Freire, P.C.C., Wex, N., Tauris, T.M., Lynch, R.S., van Kerkwijk, M.H., Kramer, M., Bassa, C., Dhillon, V.S., Driebe, T., Hessels, J.W.T., Kaspi, V.M., Kondratiev, V.I., Langer, N., Marsh, T.R., McLaughlin, M.A., Pennucci, T.T., Ransom, S.M., Stairs, I.H., van Leeuwen, J., Verbiest, J.P.W., Whelan, D.G.: A Massive Pulsar in a Compact Relativistic Binary. Science **340**, 448 (2013)
[9] Artigue, R., Barret, D., Lamb, F.K., Lo, K.H., Miller, M.C.: Testing the rotating hotspot model using X-ray burst oscillations from 4U 1636-536. MNRAS **433**, L64–L68 (2013)
[10] Avni, Y.: Mass estimates from optical-light curves for binary X-ray sources. In: R. Giacconi & R. Ruffini (ed.) Physics and Astrophysics of Neutron Stars and Black Holes, pp. 43–62 (1978)
[11] Barker, B.M., O'Connell, R.F.: Gravitational two-body problem with arbitrary masses, spins, and quadrupole moments. Phys. Rev. D **12**, 329–335 (1975)
[12] Barret, D.: Soft Lags in Neutron Star kHz Quasi-periodic Oscillations: Evidence for Reverberation? ApJ **770**, 9 (2013)
[13] Barret, D., Olive, J., Miller, M.C.: An abrupt drop in the coherence of the lower kHz quasi-periodic oscillations in 4U 1636-536. MNRAS **361**, 855–860 (2005)
[14] Barret, D., Olive, J., Miller, M.C.: Drop of coherence of the lower kilo-Hz QPO in neutron stars: Is there a link with the innermost stable circular orbit? Astronomische Nachrichten **326**, 808–811 (2005)
[15] Barret, D., Olive, J., Miller, M.C.: The coherence of kilohertz quasi-periodic oscillations in the X-rays from accreting neutron stars. MNRAS **370**, 1140–1146 (2006)
[16] Barret, D., Olive, J., Miller, M.C.: Supporting evidence for the signature of the innermost stable circular orbit in Rossi X-ray data from 4U 1636-536. MNRAS **376**, 1139–1144 (2007)
[17] Bauböck, M., Psaltis, D., Özel, F.: Narrow Atomic Features from Rapidly Spinning Neutron Stars. ApJ **766**, 87 (2013)
[18] Bauswein, A., Janka, H.T., Hebeler, K., Schwenk, A.: Equation-of-state dependence of the gravitational-wave signal from the ring-down phase of neutron-star mergers. Phys. Rev. D **86**(6), 063001 (2012)
[19] Belian, R.D., Conner, J.P., Evans, W.D.: The discovery of X-ray bursts from a region in the constellation Norma. ApJL **206**, L135–L138 (1976)

[20] Berger, E., Fong, W., Chornock, R.: An r-process Kilonova Associated with the Short-hard GRB 130603B. ApJL **774**, L23 (2013)
[21] Bernuzzi, S., Nagar, A., Thierfelder, M., Brügmann, B.: Tidal effects in binary neutron star coalescence. Phys. Rev. D **86**(4), 044030 (2012)
[22] Beznogov, M.V., Yakovlev, D.G.: Diffusion and Coulomb separation of ions in dense matter. ArXiv e-prints (2013)
[23] Bhattacharyya, S.: Measurement of neutron star parameters: A review of methods for low-mass X-ray binaries. Advances in Space Research **45**, 949–978 (2010)
[24] Bhattacharyya, S.: Ways to constrain neutron star equation of state models using relativistic disc lines. MNRAS **415**, 3247–3252 (2011)
[25] Bhattacharyya, S., Miller, M.C., Lamb, F.K.: The Shapes of Atomic Lines from the Surfaces of Weakly Magnetic Rotating Neutron Stars and Their Implications. ApJ **644**, 1085–1089 (2006)
[26] Bhattacharyya, S., Strohmayer, T.E., Miller, M.C., Markwardt, C.B.: Constraints on Neutron Star Parameters from Burst Oscillation Light Curves of the Accreting Millisecond Pulsar XTE J1814-338. ApJ **619**, 483–491 (2005)
[27] Bildsten, L., Rutledge, R.E.: Coronal X-Ray Emission from the Stellar Companions to Transiently Accreting Black Holes. ApJ **541**, 908–917 (2000)
[28] Blaes, O., Warren, O., Madau, P.: Accreting, Isolated Neutron Stars. III. Preheating of Infalling Gas and Cometary H II Regions. ApJ **454**, 370 (1995)
[29] Blaschke, D., Alvarez-Castillo, D.E., Benic, S.: Mass-radius constraints for compact stars and a critical endpoint. ArXiv e-prints (2013)
[30] Blaschke, D., Grigorian, H., Voskresensky, D.N.: Nuclear medium cooling scenario in the light of new Cas A cooling data and the 2 M_sun pulsar mass measurements. ArXiv e-prints (2013)
[31] Blinova, A.A., Bachetti, M., Romanova, M.M.: Oscillations of the Boundary Layer and High-frequency QPOs. ArXiv e-prints (2013)
[32] Bogdanov, S.: The Nearest Millisecond Pulsar Revisited with XMM-Newton: Improved Mass-radius Constraints for PSR J0437-4715. ApJ **762**, 96 (2013)
[33] Bogdanov, S., Grindlay, J.E., Rybicki, G.B.: Thermal X-Rays from Millisecond Pulsars: Constraining the Fundamental Properties of Neutron Stars. ApJ **689**, 407–415 (2008)
[34] Bondarescu, R., Wasserman, I.: Nonlinear Development of the R Mode Instability and the Maximum Rotation Rate of Neutron Stars. ArXiv e-prints (2013)
[35] Boutelier, M., Barret, D., Miller, M.C.: kHz quasi-periodic oscillations in the low-mass X-ray binary 4U 0614+09. MNRAS **399**, 1901–1906 (2009)
[36] Boutloukos, S., Lamb, F.K.: Implications of kHz QPOs for the Spin Frequencies and Magnetic Fields of Neutron Stars: New Results from Circinus X-1. In: C. Bassa, Z. Wang, A. Cumming, & V. M. Kaspi (ed.) 40 Years of Pulsars: Millisecond Pulsars, Magnetars and More, *American Institute of Physics Conference Series*, vol. 983, pp. 533–535 (2008)
[37] Boutloukos, S., Miller, M.C., Lamb, F.K.: Super-Eddington Fluxes During Thermonuclear X-ray Bursts. ApJ **720**, L15–L19 (2010)

[38] Braje, T.M., Romani, R.W., Rauch, K.P.: Light Curves of Rapidly Rotating Neutron Stars. ApJ **531**, 447–452 (2000)
[39] Broderick, A.E., Chang, P., Pfrommer, C.: The Cosmological Impact of Luminous TeV Blazars. I. Implications of Plasma Instabilities for the Intergalactic Magnetic Field and Extragalactic Gamma-Ray Background. ApJ **752**, 22 (2012)
[40] Brown, E., Gupta, S.S., Schatz, H., Möller, P., Kratz, K.: Electron capture reactions in neutron star crusts: deep heating and observational constraints. In: International Symposium on Nuclear Astrophysics - Nuclei in the Cosmos (2006)
[41] Burgay, M., D'Amico, N., Possenti, A., Manchester, R.N., Lyne, A.G., Joshi, B.C., McLaughlin, M.A., Kramer, M., Sarkissian, J.M., Camilo, F., Kalogera, V., Kim, C., Lorimer, D.R.: An increased estimate of the merger rate of double neutron stars from observations of a highly relativistic system. Nature **426**, 531–533 (2003)
[42] Burwitz, V., Zavlin, V.E., Neuhäuser, R., Predehl, P., Trümper, J., Brinkman, A.C.: The Chandra LETGS high resolution X-ray spectrum of the isolated neutron star RX J1856.5-3754. A&A **379**, L35–L38 (2001)
[43] Cackett, E.M., Miller, J.M., Bhattacharyya, S., Grindlay, J.E., Homan, J., van der Klis, M., Miller, M.C., Strohmayer, T.E., Wijnands, R.: Relativistic Iron Emission Lines in Neutron Star Low-Mass X-Ray Binaries as Probes of Neutron Star Radii. ApJ **674**, 415–420 (2008)
[44] Cadeau, C., Morsink, S.M., Leahy, D., Campbell, S.S.: Light Curves for Rapidly Rotating Neutron Stars. ApJ **654**, 458–469 (2007)
[45] Campana, S., Stella, L.: On the Bolometric Quiescent Luminosity and Luminosity Swing of Black Hole Candidate and Neutron Star Low-Mass X-Ray Transients. ApJ **541**, 849–859 (2000)
[46] Catuneanu, A., Heinke, C.O., Sivakoff, G.R., Ho, W.C.G., Servillat, M.: Mass/radius Constraints on the Quiescent Neutron Star in M13 Using Hydrogen and Helium Atmospheres. ApJ **764**, 145 (2013)
[47] Chakrabarty, D.: The spin distribution of millisecond X-ray pulsars. In: R. Wijnands, D. Altamirano, P. Soleri, N. Degenaar, N. Rea, P. Casella, A. Patruno, & M. Linares (ed.) American Institute of Physics Conference Series, *American Institute of Physics Conference Series*, vol. 1068, pp. 67–74 (2008)
[48] Chakraborty, M., Bhattacharyya, S.: Thermonuclear X-ray bursts from the 401-Hz accreting pulsar IGR J17498-2921: indication of burning in confined regions. MNRAS **422**, 2351–2356 (2012)
[49] Chang, P., Bildsten, L.: Diffusive Nuclear Burning in Neutron Star Envelopes. ApJ **585**, 464–474 (2003)
[50] Chang, P., Bildsten, L., Arras, P.: Diffusive Nuclear Burning of Helium on Neutron Stars. ApJ **723**, 719–728 (2010)
[51] Chang, P., Bildsten, L., Wasserman, I.: Formation of Resonant Atomic Lines during Thermonuclear Flashes on Neutron Stars. ApJ **629**, 998–1007 (2005)

[52] Chirenti, C., Silveira, P.R., Aguiar, O.D.: Non-Radial Oscillations of Neutron Stars and the Detection of Gravitational Waves. International Journal of Modern Physics Conference Series **18**, 48–52 (2012)
[53] Chirenti, C., Skakala, J.: The effect of magnetic fields on the r-modes of slowly rotating relativistic neutron stars. ArXiv e-prints (2013)
[54] Chirenti, C., Skákala, J., Yoshida, S.: Slowly rotating neutron stars with small differential rotation: Equilibrium models and oscillations in the Cowling approximation. Phys. Rev. D **87**(4), 044043 (2013)
[55] Chiu, H., Salpeter, E.E.: Surface X-Ray Emission from Neutron Stars. Physical Review Letters **12**, 413–415 (1964)
[56] Cook, G.B., Shapiro, S.L., Teukolsky, S.A.: Rapidly rotating neutron stars in general relativity: Realistic equations of state. ApJ **424**, 823–845 (1994)
[57] Cooper, R.L., Narayan, R.: Theoretical Models of Superbursts on Accreting Neutron Stars. ApJ **629**, 422–437 (2005)
[58] Cottam, J., Paerels, F., Mendez, M.: Gravitationally redshifted absorption lines in the X-ray burst spectra of a neutron star. Nature **420**, 51–54 (2002)
[59] Cottam, J., Paerels, F., Méndez, M., Boirin, L., Lewin, W.H.G., Kuulkers, E., Miller, J.M.: The Burst Spectra of EXO 0748-676 during a Long 2003 XMM-Newton Observation. ApJ **672**, 504–509 (2008)
[60] Damour, T., Nagar, A., Villain, L.: Measurability of the tidal polarizability of neutron stars in late-inspiral gravitational-wave signals. Phys. Rev. D **85**(12), 123007 (2012)
[61] Damour, T., Schäfer, G.: Higher-order relativistic periastron advances and binary pulsars. Nuovo Cimento B Serie **101**, 127–176 (1988)
[62] Damour, T., Taylor, J.H.: Strong-field tests of relativistic gravity and binary pulsars. Phys. Rev. D **45**, 1840–1868 (1992)
[63] Danielewicz, P., Lacey, R., Lynch, W.G.: Determination of the Equation of State of Dense Matter. Science **298**, 1592–1596 (2002)
[64] Del Pozzo, W., Li, T.G.F., Agathos, M., Van Den Broeck, C., Vitale, S.: Demonstrating the Feasibility of Probing the Neutron-Star Equation of State with Second-Generation Gravitational-Wave Detectors. Physical Review Letters **111**(7), 071101 (2013)
[65] Demorest, P.B., Pennucci, T., Ransom, S.M., Roberts, M.S.E., Hessels, J.W.T.: A two-solar-mass neutron star measured using Shapiro delay. Nature **467**, 1081–1083 (2010)
[66] Doneva, D.D., Gaertig, E., Kokkotas, K.D., Krüger, C.: Gravitational wave asteroseismology of fast rotating neutron stars with realistic equations of state. Phys. Rev. D **88**(4), 044052 (2013)
[67] Ebisuzaki, T., Sugimoto, D., Hanawa, T.: Are X-ray bursts really of super-Eddington luminosities? Pub. Astr. Soc. Jap. **36**, 551–566 (1984)
[68] Elshamouty, K.G., Heinke, C.O., Sivakoff, G.R., Ho, W.C.G., Shternin, P.S., Yakovlev, D.G., Patnaude, D.J., David, L.: Measuring the Cooling of the Neutron Star in Cassiopeia A with all Chandra X-ray Observatory Detectors. ArXiv e-prints (2013)
[69] Farhi, E., Jaffe, R.L.: Strange matter. Phys. Rev. D **30**, 2379–2390 (1984)

[70] Feroci M., e.a.: The Large Observatory for X-ray Timing (LOFT). Experimental Astronomy **34**, 415–444 (2012)
[71] Ferrari, V., Gualtieri, L., Maselli, A.: Tidal interaction in compact binaries: A post-Newtonian affine framework. Phys. Rev. D **85**(4), 044045 (2012)
[72] Foucart, F., Buchman, L., Duez, M.D., Grudich, M., Kidder, L.E., MacDonald, I., Mroue, A., Pfeiffer, H.P., Scheel, M.A., Szilagyi, B.: First direct comparison of nondisrupting neutron star-black hole and binary black hole merger simulations. Phys. Rev. D **88**(6), 064017 (2013)
[73] Frank, J., King, A., Raine, D.J.: Accretion Power in Astrophysics: Third Edition (2002)
[74] Freire, P.C.C.: Eccentric Binary Millisecond Pulsars. ArXiv e-prints (2009)
[75] Freire, P.C.C., Wex, N.: The orthometric parameterisation of the Shapiro delay and an improved test of general relativity with binary pulsars. ArXiv e-prints (2010)
[76] Fryxell, B.A., Woosley, S.E.: Finite propagation time in multidimensional thermonuclear runaways. ApJ **261**, 332–336 (1982)
[77] Fushiki, I., Lamb, D.Q.: New insights from a global view of X-ray bursts. ApJL **323**, L55–L60 (1987)
[78] Galloway, D.K., Lampe, N.: On the Consistency of Neutron-star Radius Measurements from Thermonuclear Bursts. ApJ **747**, 75 (2012)
[79] Galloway, D.K., Lin, J., Chakrabarty, D., Hartman, J.M.: Discovery of a 552 Hz Burst Oscillation in the Low-Mass X-Ray Binary EXO 0748-676. ApJ **711**, L148–L151 (2010)
[80] García, F., Zhang, G., Méndez, M.: The cooling phase of Type I X-ray bursts observed with RXTE in 4U 1820-30 does not follow the canonical $F \propto T^4$ relation. MNRAS **429**, 3266–3271 (2013)
[81] Gendreau, K.C., Arzoumanian, Z., Okajima, T.: The Neutron star Interior Composition ExploreR (NICER): an Explorer mission of opportunity for soft x-ray timing spectroscopy. In: Society of Photo-Optical Instrumentation Engineers (SPIE) Conference Series, *Society of Photo-Optical Instrumentation Engineers (SPIE) Conference Series*, vol. 8443 (2012)
[82] Grindlay, J., Gursky, H., Schnopper, H., Parsignault, D.R., Heise, J., Brinkman, A.C., Schrijver, J.: Discovery of intense X-ray bursts from the globular cluster NGC 6624. ApJL **205**, L127–L130 (1976)
[83] Guillot, S., Rutledge, R.E., Bildsten, L., Brown, E.F., Pavlov, G.G., Zavlin, V.E.: X-ray spectral identification of three candidate quiescent low-mass X-ray binaries in the globular cluster NGC 6304. MNRAS **392**, 665–681 (2009)
[84] Guillot, S., Rutledge, R.E., Brown, E.F.: Neutron Star Radius Measurement with the Quiescent Low-Mass X-ray Binary U24 in NGC 6397. ArXiv e-prints (2010)
[85] Guillot, S., Servillat, M., Webb, N.A., Rutledge, R.E.: Measurement of the Radius of Neutron Stars with High Signal-to-noise Quiescent Low-mass X-Ray Binaries in Globular Clusters. ApJ **772**, 7 (2013)
[86] Güver, T., Wroblewski, P., Camarota, L., Özel, F.: The Mass and Radius of the Neutron Star in 4U 1820–30. ApJ **719**, 1807–1812 (2010)

[87] Hartman, J.M., Patruno, A., Chakrabarty, D., Markwardt, C.B., Morgan, E.H., van der Klis, M., Wijnands, R.: A Decade of Timing an Accretion-powered Millisecond Pulsar: The Continuing Spin Down and Orbital Evolution of SAX J1808.4-3658. ApJ **702**, 1673–1678 (2009)
[88] Haskell, B., Degenaar, N., Ho, W.C.G.: Constraining the physics of the r-mode instability in neutron stars with X-ray and ultraviolet observations. MNRAS **424**, 93–103 (2012)
[89] Haskell, B., Patruno, A.: Spin Equilibrium with or without Gravitational Wave Emission: The Case of XTE J1814-338 and SAX J1808.4-3658. ApJL **738**, L14 (2011)
[90] Hebeler, K., Lattimer, J.M., Pethick, C.J., Schwenk, A.: Constraints on neutron star radii based on chiral effective field theory interactions. ArXiv e-prints (2010)
[91] Hebeler, K., Lattimer, J.M., Pethick, C.J., Schwenk, A.: Equation of State and Neutron Star Properties Constrained by Nuclear Physics and Observation. ApJ **773**, 11 (2013)
[92] Heinke, C.O.: Constraints on physics of neutron stars from X-ray observations. Journal of Physics Conference Series **432**(1), 012001 (2013)
[93] Hessels, J.W.T., Ransom, S.M., Stairs, I.H., Freire, P.C.C., Kaspi, V.M., Camilo, F.: A Radio Pulsar Spinning at 716 Hz. Science **311**, 1901–1904 (2006)
[94] Hinderer, T., Lackey, B.D., Lang, R.N., Read, J.S.: Tidal deformability of neutron stars with realistic equations of state and their gravitational wave signatures in binary inspiral. Phys. Rev. D **81**(12), 123016 (2010)
[95] Ho, W.C.G., Heinke, C.O.: A neutron star with a carbon atmosphere in the Cassiopeia A supernova remnant. Nature **462**, 71–73 (2009)
[96] Hoffman, J.A., Cominsky, L., Lewin, W.H.G.: Repeatable, multiple-peaked structure in Type I X-ray bursts. ApJL **240**, L27–L31 (1980)
[97] Hotokezaka, K., Kyutoku, K., Shibata, M.: Exploring tidal effects of coalescing binary neutron stars in numerical relativity. Phys. Rev. D **87**(4), 044001 (2013)
[98] Hsu, S.D.H., Reeb, D.: On the Sign Problem in Dense QCD. International Journal of Modern Physics A **25**, 53–67 (2010)
[99] Jonker, P.G., Steeghs, D., Chakrabarty, D., Juett, A.M.: The Cold Neutron Star in the Soft X-Ray Transient 1H 1905+000. ApJ **665**, L147–L150 (2007)
[100] Jonker, P.G., Steeghs, D., Nelemans, G., van der Klis, M.: The radial velocity of the companion star in the low-mass X-ray binary 2S 0921-630: limits on the mass of the compact object. MNRAS **356**, 621–626 (2005)
[101] Joss, P.C.: X-ray bursts and neutron-star thermonuclear flashes. Nature **270**, 310–314 (1977)
[102] Kaaret, P., Prieskorn, Z., in 't Zand, J.J.M., Brandt, S., Lund, N., Mereghetti, S., Götz, D., Kuulkers, E., Tomsick, J.A.: Evidence of 1122 Hz X-Ray Burst Oscillations from the Neutron Star X-Ray Transient XTE J1739-285. ApJl **657**, L97–L100 (2007)

[103] King, A.R., Kolb, U.: The evolution of black hole mass and angular momentum. MNRAS **305**, 654–660 (1999)
[104] Kiziltan, B., Kottas, A., De Yoreo, M., Thorsett, S.E.: The Neutron Star Mass Distribution. ArXiv e-prints (2013)
[105] Klähn, T., Blaschke, D., Typel, S., van Dalen, E.N.E., Faessler, A., Fuchs, C., Gaitanos, T., Grigorian, H., Ho, A., Kolomeitsev, E.E., Miller, M.C., Röpke, G., Trümper, J., Voskresensky, D.N., Weber, F., Wolter, H.H.: Constraints on the high-density nuclear equation of state from the phenomenology of compact stars and heavy-ion collisions. Phys. Rev. C **74**(3), 035,802 (2006)
[106] Kramer, M., Stairs, I.H.: The Double Pulsar. ARA&A **46**, 541–572 (2008)
[107] Kulkarni, A.K., Romanova, M.M.: Variability Profiles of Millisecond X-Ray Pulsars: Results of Pseudo-Newtonian Three-dimensional Magnetohydrodynamic Simulations. ApJ **633**, 349–357 (2005)
[108] Kulkarni, A.K., Romanova, M.M.: Possible quasi-periodic oscillations from unstable accretion: 3D magnetohydrodynamic simulations. MNRAS **398**, 701–714 (2009)
[109] Kurkela, A., Romatschke, P., Vuorinen, A.: Cold quark matter. Phys. Rev. D **81**(10), 105021 (2010)
[110] Lackey, B.D., Kyutoku, K., Shibata, M., Brady, P.R., Friedman, J.L.: Extracting equation of state parameters from black hole-neutron star mergers: Nonspinning black holes. Phys. Rev. D **85**(4), 044061 (2012)
[111] Lackey, B.D., Kyutoku, K., Shibata, M., Brady, P.R., Friedman, J.L.: Extracting equation of state parameters from black hole-neutron star mergers: aligned-spin black holes and a preliminary waveform model. ArXiv e-prints (2013)
[112] Lackey, B.D., Nayyar, M., Owen, B.J.: Observational constraints on hyperons in neutron stars. Phys. Rev. D **73**(2), 024,021 (2006)
[113] Lamb, D.Q., Lamb, F.K.: Nuclear burning in accreting neutron stars and X-ray bursts. ApJ **220**, 291–302 (1978)
[114] Lamb, F.K., Boutloukos, S., Van Wassenhove, S., Chamberlain, R.T., Lo, K.H., Clare, A., Yu, W., Miller, M.C.: A Model for the Waveform Behavior of Accreting Millisecond X-Ray Pulsars: Nearly Aligned Magnetic Fields and Moving Emission Regions. ApJ **706**, 417–435 (2009)
[115] Lamb, F.K., Boutloukos, S., Van Wassenhove, S., Chamberlain, R.T., Lo, K.H., Miller, M.C.: Origin of Intermittent Accretion-Powered X-ray Oscillations in Neutron Stars with Millisecond Spin Periods. ApJL **705**, L36–L39 (2009)
[116] Landau, L.D., Lifshitz, E.M.: Quantum mechanics (1965)
[117] Lattimer, J.M.: The Nuclear Equation of State and Neutron Star Masses. Annual Review of Nuclear and Particle Science **62**, 485–515 (2012)
[118] Lattimer, J.M., Prakash, M.: Neutron Star Structure and the Equation of State. ApJ **550**, 426–442 (2001)
[119] Lattimer, J.M., Prakash, M.: Equation of state, neutron stars and exotic phases. Nuclear Physics A **777**, 479–496 (2006)

[120] Lattimer, J.M., Prakash, M.: What a Two Solar Mass Neutron Star Really Means. ArXiv e-prints (2010)
[121] Lattimer, J.M., Schutz, B.F.: Constraining the Equation of State with Moment of Inertia Measurements. ApJ **629**, 979–984 (2005)
[122] Lattimer, J.M., Steiner, A.W.: Neutron Star Masses and Radii from Quiescent Low-Mass X-ray Binaries. ArXiv e-prints (2013)
[123] Leahy, D.A., Morsink, S.M., Chou, Y.: Constraints on the Mass and Radius of the Neutron Star XTE J1807-294. ApJ **742**, 17 (2011)
[124] Lewin, W.H.G., Hoffman, J.A., Doty, J., Hearn, D.R., Clark, G.W., Jernigan, J.G., Li, F.K., McClintock, J.E., Richardson, J.: Discovery of X-ray bursts from several sources near the galactic centre. MNRAS **177**, 83P–92P (1976)
[125] Lewin, W.H.G., van Paradijs, J., Taam, R.E.: X-Ray Bursts. Space Science Reviews **62**, 223–389 (1993)
[126] Lo, K.H., Miller, M.C., Bhattacharyya, S., Lamb, F.K.: Determining Neutron Star Masses and Radii Using Energy-resolved Waveforms of X-Ray Burst Oscillations. ApJ **776**, 19 (2013)
[127] Long, M., Romanova, M.M., Lovelace, R.V.E.: Accretion to stars with non-dipole magnetic fields. MNRAS **374**, 436–444 (2007)
[128] Lovelace, R.V.E., Romanova, M.M.: Three Disk Oscillation Modes of Rotating Magnetized Neutron Stars. ApJ **670**, L13–L16 (2007)
[129] Lyne, A.G., Burgay, M., Kramer, M., Possenti, A., Manchester, R.N., Camilo, F., McLaughlin, M.A., Lorimer, D.R., D'Amico, N., Joshi, B.C., Reynolds, J., Freire, P.C.C.: A Double-Pulsar System: A Rare Laboratory for Relativistic Gravity and Plasma Physics. Science **303**, 1153–1157 (2004)
[130] Mahmoodifar, S., Strohmayer, T.: Upper Bounds on r-mode Amplitudes from Observations of Low-mass X-Ray Binary Neutron Stars. ApJ **773**, 140 (2013)
[131] Majczyna, A., Madej, J.: Mass and Radius Determination for the Neutron Star in X-ray Burst Source 4U/MXB 1728-34. Acta. Astronom. **55**, 349–366 (2005)
[132] Manchester, R.N.: Radio Emission Properties of Pulsars. In: W. Becker (ed.) Astrophysics and Space Science Library, *Astrophysics and Space Science Library*, vol. 357, pp. 19–39 (2009)
[133] McClintock, J.E., Narayan, R., Gou, L., Liu, J., Penna, R.F., Steiner, J.F.: Measuring the Spins of Stellar Black Holes: A Progress Report. In: A. Comastri, L. Angelini, & M. Cappi (ed.) American Institute of Physics Conference Series, *American Institute of Physics Conference Series*, vol. 1248, pp. 101–106 (2010)
[134] McClintock, J.E., Remillard, R.A.: The X-ray nova Centaurus X-4 - Comparisons with A0620 - 00. ApJ **350**, 386–394 (1990)
[135] McLaughlin, D.B.: The spectrum of Nova Herculis. Publications of Michigan Observatory **6**, 107–214 (1937)
[136] Méndez, M.: On the maximum amplitude and coherence of the kilohertz quasi-periodic oscillations in low-mass X-ray binaries. MNRAS **371**, 1925–1938 (2006)

[137] Méndez, M., Belloni, T.: Is there a link between the neutron-star spin and the frequency of the kilohertz quasi-periodic oscillations? MNRAS **381**, 790–796 (2007)
[138] Méndez, M., van der Klis, M., Ford, E.C., Wijnands, R., van Paradijs, J.: Dependence of the Frequency of the Kilohertz Quasi-periodic Oscillationson X-Ray Count Rate and Colors in 4U 1608-52. ApJ **511**, L49–L52 (1999)
[139] Miller, J.M.: Relativistic X-Ray Lines from the Inner Accretion Disks Around Black Holes. ARA&A **45**, 441–479 (2007)
[140] Miller, M.C.: Model atmospheres for neutron stars. MNRAS **255**, 129–145 (1992)
[141] Miller, M.C.: Prompt Mergers of Neutron Stars with Black Holes. ApJl **626**, L41–L44 (2005)
[142] Miller, M.C., Boutloukos, S., Lo, K.H., Lamb, F.K.: Implications of high-precision spectra of thermonuclear X-ray bursts for determining neutron star masses and radii. In: Fast X-ray Timing and Spectroscopy at Extreme Count Rates (HTRS 2011) (2011)
[143] Miller, M.C., Lamb, F.K.: Bounds on the Compactness of Neutron Stars from Brightness Oscillations during X-Ray Bursts. ApJL **499**, L37+ (1998)
[144] Miller, M.C., Lamb, F.K., Cook, G.B.: Effects of Rapid Stellar Rotation on Equation-of-State Constraints Derived from Quasi-periodic Brightness Oscillations. ApJ **509**, 793–801 (1998)
[145] Miller, M.C., Lamb, F.K., Psaltis, D.: Sonic-Point Model of Kilohertz Quasi-periodic Brightness Oscillations in Low-Mass X-Ray Binaries. ApJ **508**, 791–830 (1998)
[146] Miller, M.C., Neuhauser, D.: Atoms in very strong magnetic fields. MNRAS **253**, 107–122 (1991)
[147] Morsink, S.M., Leahy, D.A.: Multi-epoch Analysis of Pulse Shapes from the Neutron Star SAX J1808.4-3658. ApJ **726**, 56 (2011)
[148] Muno, M.P., Özel, F., Chakrabarty, D.: The Energy Dependence of Millisecond Oscillations in Thermonuclear X-Ray Bursts. ApJ **595**, 1066–1076 (2003)
[149] Nandra, K., Barret, D., Barcons, X., Fabian, A., den Herder, J.W., Piro, L., Watson, M., Adami, C., Aird, J., Afonso, J.M., et al.: The Hot and Energetic Universe: A White Paper presenting the science theme motivating the Athena+ mission. ArXiv e-prints (2013)
[150] Nath, N.R., Strohmayer, T.E., Swank, J.H.: Bounds on Compactness for Low-Mass X-Ray Binary Neutron Stars from X-Ray Burst Oscillations. ApJ **564**, 353–360 (2002)
[151] Nomoto, K.: Evolution of 8-10 solar mass stars toward electron capture supernovae. I - Formation of electron-degenerate O + NE + MG cores. ApJ **277**, 791–805 (1984)
[152] Oppenheimer, J.R., Volkoff, G.M.: On Massive Neutron Cores. Physical Review **55**, 374–381 (1939)
[153] Özel, F.: Surface emission from neutron stars and implications for the physics of their interiors. Reports on Progress in Physics **76**(1), 016901 (2013)

[154] Özel, F., Psaltis, D.: Reconstructing the neutron-star equation of state from astrophysical measurements. Phys. Rev. D **80**(10), 103,003 (2009)
[155] Paczynski, B.: Models of X-ray bursters with radius expansion. ApJ **267**, 315–321 (1983)
[156] Page, D., Applegate, J.H.: The cooling of neutron stars by the direct URCA process. ApJl **394**, L17–L20 (1992)
[157] Page, D., Geppert, U., Weber, F.: The cooling of compact stars. Nuclear Physics A **777**, 497–530 (2006)
[158] Page, D., Lattimer, J.M., Prakash, M., Steiner, A.W.: Neutrino Emission from Cooper Pairs and Minimal Cooling of Neutron Stars. ApJ **707**, 1131–1140 (2009)
[159] Page, D., Prakash, M., Lattimer, J.M., Steiner, A.W.: Rapid Cooling of the Neutron Star in Cassiopeia A Triggered by Neutron Superfluidity in Dense Matter. Physical Review Letters **106**(8), 081101 (2011)
[160] Page, D., Reddy, S.: Dense Matter in Compact Stars: Theoretical Developments and Observational Constraints. Annual Review of Nuclear and Particle Science **56**, 327–374 (2006)
[161] Papitto, A., Riggio, A., Burderi, L., Di Salvo, T., D'Aí, A., Iaria, R.: Spin down during quiescence of the fastest known accretion-powered pulsar. ArXiv e-prints (2010)
[162] Patruno, A., Haskell, B., D'Angelo, C.: Gravitational Waves and the Maximum Spin Frequency of Neutron Stars. ApJ **746**, 9 (2012)
[163] Peters, P.C.: Gravitational Radiation and the Motion of Two Point Masses. Physical Review **136**, 1224–1232 (1964)
[164] Piekarewicz, J.: Neutron Skins and Neutron Stars. ArXiv e-prints (2013)
[165] Podsiadlowski, P., Dewi, J.D.M., Lesaffre, P., Miller, J.C., Newton, W.G., Stone, J.R.: The double pulsar J0737-3039: testing the neutron star equation of state. MNRAS **361**, 1243–1249 (2005)
[166] Posselt, B., Pavlov, G.G., Suleimanov, V., Kargaltsev, O.: New constraints on the cooling of the Central Compact Object in Cas A. ArXiv e-prints (2013)
[167] Psaltis, D.: Testing general metric theories of gravity with bursting neutron stars. Phys. Rev. D **77**(6), 064,006 (2008)
[168] Rajagopal, M., Romani, R.W., Miller, M.C.: Magnetized Iron Atmospheres for Neutron Stars. ApJ **479**, 347–356 (1997)
[169] Ray, P.S., Phlips, B.F., Wood, K.S., Chakrabarty, D., Remillard, R.A., Wilson-Hodge, C.A.: The Advanced X-ray Timing Array (AXTAR): A US MIDEX Mission Concept. ArXiv e-prints (2011)
[170] Read, J.S., Baiotti, L., Creighton, J.D.E., Friedman, J.L., Giacomazzo, B., Kyutoku, K., Markakis, C., Rezzolla, L., Shibata, M., Taniguchi, K.: Matter effects on binary neutron star waveforms. Phys. Rev. D **88**(4), 044042 (2013)
[171] Romani, R.W.: Model atmospheres for cooling neutron stars. ApJ **313**, 718–726 (1987)
[172] Romani, R.W., Filippenko, A.V., Silverman, J.M., Cenko, S.B., Greiner, J., Rau, A., Elliott, J., Pletsch, H.J.: PSR J1311-3430: A Heavyweight Neutron Star with a Flyweight Helium Companion. ApJL **760**, L36 (2012)

[173] Romanova, M.M., Kulkarni, A., Long, M., Lovelace, R.V.E., Wick, J.V., Ustyugova, G.V., Koldoba, A.V.: 2D and 3D MHD simulations of disk accretion by rotating magnetized stars: Search for variability. Advances in Space Research **38**, 2887–2892 (2006)
[174] Romanova, M.M., Kulkarni, A.K., Lovelace, R.V.E.: Unstable Disk Accretion onto Magnetized Stars: First Global Three-dimensional Magnetohydrodynamic Simulations. ApJ **673**, L171–L174 (2008)
[175] Romanova, M.M., Ustyugova, G.V., Koldoba, A.V., Lovelace, R.V.E.: Three-dimensional Simulations of Disk Accretion to an Inclined Dipole. II. Hot Spots and Variability. ApJ **610**, 920–932 (2004)
[176] Romanova, M.M., Ustyugova, G.V., Koldoba, A.V., Wick, J.V., Lovelace, R.V.E.: Three-dimensional Simulations of Disk Accretion to an Inclined Dipole. I. Magnetospheric Flows at Different Θ. ApJ **595**, 1009–1031 (2003)
[177] Rossiter, R.A.: On the detection of an effect of rotation during eclipse in the velocity of the brigher component of beta Lyrae, and on the constancy of velocity of this system. ApJ **60**, 15–21 (1924)
[178] Rutledge, R.E., Bildsten, L., Brown, E.F., Pavlov, G.G., Zavlin, V.E.: The Quiescent X-Ray Spectrum of the Neutron Star in Centaurus X-4 Observed with Chandra/ACIS-S. ApJ **551**, 921–928 (2001)
[179] Rybicki, G.B., Lightman, A.P.: Radiative Processes in Astrophysics (1986)
[180] Schwab, J., Podsiadlowski, P., Rappaport, S.: Further Evidence for the Bimodal Distribution of Neutron-star Masses. ApJ **719**, 722–727 (2010)
[181] Sedrakian, A.: The physics of dense hadronic matter and compact stars. Progress in Particle and Nuclear Physics **58**, 168–246 (2007)
[182] Servillat, M., Heinke, C.O., Ho, W.C.G., Grindlay, J.E., Hong, J., van den Berg, M., Bogdanov, S.: Neutron star atmosphere composition: the quiescent, low-mass X-ray binary in the globular cluster M28. MNRAS **423**, 1556–1561 (2012)
[183] Shternin, P.S., Yakovlev, D.G., Heinke, C.O., Ho, W.C.G., Patnaude, D.J.: Cooling neutron star in the Cassiopeia A supernova remnant: evidence for superfluidity in the core. MNRAS **412**, L108–L112 (2011)
[184] Smale, A.P.: A Second Intense Burst with Photospheric Radius Expansion from X2127+119 in M15. ApJ **562**, 957–962 (2001)
[185] Spitkovsky, A., Levin, Y., Ushomirsky, G.: Propagation of Thermonuclear Flames on Rapidly Rotating Neutron Stars: Extreme Weather during Type I X-Ray Bursts. ApJ **566**, 1018–1038 (2002)
[186] Stairs, I.H.: Testing General Relativity with Pulsar Timing. Living Reviews in Relativity **6**, 5 (2003)
[187] Steiner, A.W., Lattimer, J.M., Brown, E.F.: The Equation of State from Observed Masses and Radii of Neutron Stars. ApJ **722**, 33–54 (2010)
[188] Stergioulas, N.: Rotating Stars in Relativity. Living Reviews in Relativity **6**, 3 (2003)
[189] Suleimanov, V., Poutanen, J., Revnivtsev, M., Werner, K.: A Neutron Star Stiff Equation of State Derived from Cooling Phases of the X-Ray Burster 4U 1724-307. ApJ **742**, 122 (2011)

[190] Suleimanov, V., Poutanen, J., Werner, K.: X-ray bursting neutron star atmosphere models using an exact relativistic kinetic equation for Compton scattering. A&A **545**, A120 (2012)
[191] Taam, R.E., Picklum, R.E.: Nuclear fusion and carbon flashes on neutron stars. ApJ **224**, 210–216 (1978)
[192] Taam, R.E., Woosley, S.E., Weaver, T.A., Lamb, D.Q.: Successive X-ray bursts from accreting neutron stars. ApJ **413**, 324–332 (1993)
[193] Tanvir, N.R., Levan, A.J., Fruchter, A.S., Hjorth, J., Hounsell, R.A., Wiersema, K., Tunnicliffe, R.L.: A 'kilonova' associated with the short-duration γ-ray burst GRB130603B. Nature **500**, 547–549 (2013)
[194] Tomsick, J.A., Muterspaugh, M.W.: Masses of Neutron Stars in High-Mass X-ray Binaries with Optical Astrometry. ArXiv e-prints (2010)
[195] Troyer, M., Wiese, U.: Computational Complexity and Fundamental Limitations to Fermionic Quantum Monte Carlo Simulations. Physical Review Letters **94**(17), 170,201–+ (2005)
[196] Ushomirsky, G., Cutler, C., Bildsten, L.: Deformations of accreting neutron star crusts and gravitational wave emission. MNRAS **319**, 902–932 (2000)
[197] Ushomirsky, G., Rutledge, R.E.: Time-variable emission from transiently accreting neutron stars in quiescence due to deep crustal heating. MNRAS **325**, 1157–1166 (2001)
[198] Van Den Broeck, C.: Astrophysics, cosmology, and fundamental physics with compact binary coalescence and the Einstein Telescope. ArXiv e-prints (2013)
[199] van der Sluys, M., Mandel, I., Raymond, V., Kalogera, V., Röver, C., Christensen, N.: Parameter estimation for signals from compact binary inspirals injected into LIGO data. Classical and Quantum Gravity **26**(20), 204,010 (2009)
[200] van Eysden, C.A., Melatos, A.: Gravitational radiation from pulsar glitches. Classical and Quantum Gravity **25**(22), 225,020–+ (2008)
[201] van Kerkwijk, M.H., Breton, R.P., Kulkarni, S.R.: Evidence for a Massive Neutron Star from a Radial-velocity Study of the Companion to the Black-widow Pulsar PSR B1957+20. ApJ **728**, 95 (2011)
[202] van Kerkwijk, M.H., Kaplan, D.L.: Isolated neutron stars: magnetic fields, distances,and spectra. Astr. Sp. Sci. **308**, 191–201 (2007)
[203] van Paradijs, J.: Possible observational constraints on the mass-radius relation of neutron stars. ApJ **234**, 609–611 (1979)
[204] Venumadhav, T., Zimmerman, A., Hirata, C.M.: The stability of tidally deformed neutron stars to three- and four-mode coupling. ArXiv e-prints (2013)
[205] Villarreal, A.R., Strohmayer, T.E.: Discovery of the Neutron Star Spin Frequency in EXO 0748-676. ApJL **614**, L121–L124 (2004)
[206] Walter, F.M., Eisenbeiss, T., Lattimer, J.M., Kim, B., Hambaryan, V., Neuhaeuser, R.: Revisiting the Parallax of the Isolated Neutron Star RX J185635-3754 Using HST/ACS Imaging. ArXiv e-prints (2010)
[207] Walter, F.M., Lattimer, J.M.: A Revised Parallax and Its Implications for RX J185635-3754. ApJl **576**, L145–L148 (2002)

[208] Watts, A.L.: Thermonuclear Burst Oscillations. Ann. Rev. Astron. Astrop. **50**, 609–640 (2012)
[209] Webb, N.A., Barret, D.: Constraining the Equation of State of Supranuclear Dense Matter from XMM-Newton Observations of Neutron Stars in Globular Clusters. ApJ **671**, 727–733 (2007)
[210] Weber, F., Negreiros, R., Rosenfield, P.: Neutron Star Interiors and the Equation of State of Superdense Matter. ArXiv e-prints (2007)
[211] Weinberg, N., Miller, M.C., Lamb, D.Q.: Oscillation Waveforms and Amplitudes from Hot Spots on Neutron Stars. ApJ **546**, 1098–1106 (2001)
[212] Woosley, S.E., Heger, A., Weaver, T.A.: The evolution and explosion of massive stars. Reviews of Modern Physics **74**, 1015–1071 (2002)
[213] Woosley, S.E., Taam, R.E.: Gamma-ray bursts from thermonuclear explosions on neutron stars. Nature **263**, 101–103 (1976)
[214] Yagi, K., Yunes, N.: I-Love-Q relations in neutron stars and their applications to astrophysics, gravitational waves, and fundamental physics. Phys. Rev. D **88**(2), 023009 (2013)
[215] Yakovlev, D.G., Pethick, C.J.: Neutron Star Cooling. ARA&A **42**, 169–210 (2004)
[216] Zhang, C.M., Wang, J., Zhao, Y.H., Yin, H.X., Song, L.M., Menezes, D.P., Wickramasinghe, D.T., Ferrario, L., Chardonnet, P.: Study of measured pulsar masses and their possible conclusions. A&A **527**, A83 (2011)
[217] Zhang, G., Mendez, M., Belloni, T.M., Homan, J.: Coherent oscillations and the evolution of the emission area in the decaying phase of radius-expansion bursts from 4U 1636-53. ArXiv e-prints (2012)
[218] Zhang, W., Smale, A.P., Strohmayer, T.E., Swank, J.H.: Correlation between Energy Spectral States and Fast Time Variability and Further Evidence for the Marginally Stable Orbit in 4U 1820-30. ApJ **500**, L171–174 (1998)